2-47-61-1 • JUNE 1961

TECHNICAL REPORT: FLIGHT SCIENCES

MINIMUM WEIGHT ANALYSES FOR FOUR TYPES OF STIFFENED, FLAT, COMPRESSION PANELS AND THEIR RELATIVE EFFICIENCY

2-47-61-1 • JUNE 1961

2-47-61-1

TECHNICAL REPORT: FLIGHT SCIENCES

MINIMUM WEIGHT ANALYSES FOR FOUR TYPES OF STIFFENED, FLAT, COMPRESSION PANELS AND THEIR RELATIVE EFFICIENCY

by

A. B. BURNS

R. F. CRAWFORD

WORK CARRIED OUT AS PART OF THE LOCKHEED GENERAL RESEARCH PROGRAM AND U.S. AIR FORCE CONTRACT NO. AF 33(616)-6905

Lockheed

MISSILES and SPACE DIVISION

LOCKHEED AIRCRAFT CORPORATION • SUNNYVALE, CALIF.

FOREWORD

This technical report provides methods for the minimum weight design of four types of stiffened flat plates. It is an outgrowth of work carried out as part of the Lockheed General Research Program, and under additional support from U.S. Air Force Contract No. AF 33(616)-6905.

ABSTRACT

Minimum weight analyses for four types of flat compression panel construction, each of which is stiffened parallel to the direction of loading, are described and solutions presented and compared. These solutions indicate the most efficient distribution of material between skin and stiffeners for each construction as a function of the magnitude of the load. Similar analyses, solutions and comparisons applicable to wide columns are presented in an appendix. Design charts for both the flat compression panel construction and wide column construction are given, comparing less efficient geometries to the minimum weight geometries.

CONTENTS

Section		Page
	FOREWORD	iii
	ABSTRACT	v
	LIST OF ILLUSTRATIONS	ix
	NOMENCLATURE	xi
1.	INTRODUCTION	1-1
2.	MINIMUM WEIGHT ANALYSES	2-1
	2.1 Analysis of Zee-Stiffened Flat Panels in Compression	2-1
	2.2 Analysis of Unflanged, Integrally-Stiffened Flat Panels	2-22
	2.3 Analysis of Truss-Core Semi-Sandwich Flat Panels	2-28
	2.4 Analysis of Truss-Core Sandwich Flat Panels	2-34
3.	RELATIVE EFFICIENCIES OF THE SEVERAL TYPES OF PANEL CONSTRUCTION	3-1
4.	CONCLUSIONS	4-1
5.	REFERENCES	5-1
Appendix		
A.	EFFICIENCY OF FLAT, UNSTIFFENED PLATES IN COMPRESSION	A-1
B.	A SUMMARY OF WIDE COLUMN MINIMUM WEIGHT ANALYSES FOR STIFFENED CONSTRUCTIONS	B-1

LIST OF ILLUSTRATIONS

Figure		Page
1-1	Multi-Rib Wing Box Construction	1-2
1-2a	Multi-Spar Wing Box Construction	1-2
1-2b	Rib-Spar Wing Box Construction	1-3
2-1	Cross-Sectional Geometry of a Zee-Stiffened Panel	2-3
2-2a	Efficiency Chart for Zee-Stiffened Flat Panels in Compression (Stiffeners Parallel to Load)	2-12
2-2b	Efficiency Chart for Zee-Stiffened Flat Panels in Compression (Stiffeners Parallel to Load) (Continuation of Fig. 2-2a)	2-13
2-3	Auxiliary Design Chart for Zee-Stiffened Flat Panels in Compression	2-14
2-4	Typical Example of the Variation of $\sigma/\bar{\eta}$ with σ	2-16
2-5	Cross-Sectional Geometry of an Unflanged, Integrally-Stiffened Panel	2-22
2-6a	Efficiency Chart for Unflanged, Integrally-Stiffened Flat Panels in Compression (Stiffeners Parallel to Load)	2-25
2-6b	Efficiency Chart for Unflanged, Integrally-Stiffened Flat Panels in Compression (Stiffeners Parallel to Load) (Continuation of Fig. 2.6a)	2-26
2-7	Auxiliary Design Chart for Unflanged, Integrally-Stiffened Flat Panels in Compression	2-27
2-8	Cross-Sectional Geometry of a Truss-Core Semi-Sandwich Panel	2-28
2-9	Efficiency Chart for Truss-Core Semi-Sandwich Panels (Corrugations Parallel to Load)	2-32
2-10	Comparison Between Exact and Approximate Truss-Core Semi-Sandwich Panel Solutions at High Loading-Material Indexes (Corrugations Parallel to Load)	2-35
2-11	Efficiency Chart for Truss-Core Sandwich Panels (Corrugations Parallel to Load)	2-37
3-1	Comparison of the Minimum Weight Envelopes of the Several Types of Stiffened Panel Construction when Subjected to a Compression Load in the Direction of the Stiffening Elements	3-3

NOMENCLATURE

a	length of panel parallel to load
A	area of stiffener cross-section
b	width of panel
b_c	width of sandwich core element
b_f	width of sandwich or semi-sandwich facing sheet element; width of stiffener flange element.
b_s	width of sheet element between $\mathbb{Q}_L$ - $\mathbb{Q}_L$ stiffeners
b_w	height of stiffener web element
c	restraint coefficient
D	flexural stiffness of facing sheet per unit width, $\frac{Et_s^3}{12(1-\mu^2)}$
E	Young's modulus
E_T	tangent modulus
$\mathcal{E}$	efficiency factor
$F_{0.7}$	seven-tenths secant yield stress; the stress at the intersection between the compressive stress-strain curve and a secant line through the origin having a slope equal to $0.7\ E_c$.
F_{cy}	compressive yield stress at which permanent strain equals 0.002 in/in.
I	bending moment of inertia of stiffener cross-section taken about the stiffener centroidal axis.
K_F	buckling coefficient for compressive local buckling of a stiffener flange element.
K_G	buckling coefficient for compressive general buckling of a stiffened panel.
K_S	buckling coefficient for compressive local buckling of a sheet element of width b_s .
K_W	buckling coefficient for compressive local buckling of a stiffener web element.
K_X	buckling coefficient for compressive local buckling of truss-core sandwich or semi-sandwich.

l	length of a wide column
m	reciprocal of the slope of the straight line portion of a minimum weight envelope when plotted on log-log paper as $\bar{t}/b$ versus $N_x/b\bar{\eta}E$.
N	number of bays in a conventionally stiffened panel design.
N_x	compressive loading on an unstiffened panel or a stiffened panel in the direction of the stiffening elements per unit width.
n	shape factor defining the knee of the compressive stress-strain curve.
t	thickness of a flat unstiffened plate
$\bar{t}$	equivalent flat-plate thickness of the stiffened panel for weight purposes.
t_c	thickness of core material in sandwich or semi-sandwich panels.
t_f	thickness of facing sheet in sandwich or semi-snadwich panels; thickness of stiffener flange element.
t_s	thickness of sheet or skin element between $\mathcal{C}_L$ - $\mathcal{C}_L$ stiffeners
t_w	thickness of stiffener web element
W	weight of flat plate per unit length
$\bar{z}$	distance from midsurface of skin to stiffener centroidal axis
Z_{nq}	constant; equal to 0.50 for panel with one stiffener, 0.67 for panel with two stiffeners.
$\bar{\eta}$	effective plasticity reduction factor
η_G	plasticity reduction factor for general instability
η_L	plasticity reduction factor for local instability
η_T	ratio of tangent modulus, E_T , to Young's modulus.
θ	angle between facing and core elements in truss-core sandwich or semi-sandwich
μ	Poisson's ratio
σ	compressive stress, equal to $N_x/\bar{t}$
ρ	density; radius of gyration

Subscripts

cr	critical
G	general
L	local
c	core

f	facing, flange
s	sheet or skin
w	web

Section 1
INTRODUCTION

The minimum weight analysis of missile and spacecraft structures is of major importance in design because it can lead directly to increased performance by minimizing structural weight. This report presents minimum weight analyses for the following types of construction subjected to a compressive load acting parallel to stiffening elements:

(1) Zee-stiffened flat panel
(2) Unflanged integrally-stiffened flat panel
(3) Truss-core, semi-sandwich flat panel
(4) Truss-core sandwich flat panel

This report is concerned with the choice of (1) the most efficient type of construction and (2) the most efficient geometry in this construction to carry the applied load. While these two factors contributing to minimum weight design make up the body of discussion, a third factor, the choice of material for minimum weight performance. is treated in Appendix A for the case of an unstiffened plate in compression. It may be shown that the effects on efficiency of choice of material as determined for unstiffened plates are qualitatively the same for stiffened panels.

For most compression panel constructions, two types of instability analyses may be considered. They are: (1) general instability of the composite structure, and (2) local instability of any of the elements of the composite structure. It should be noted that the term "panel" is used here to define a plate or composite construction having support along the unloaded edges. For general instability analysis, appropriate boundary conditions must be imposed; e.g., if the unloaded edges are simply supported,

general instability may be calculated on the basis of orthotropic plate theory; if free, general instability may be calculated on the basis of Euler or wide-Column theory.

There are minimum weight analyses available in the literature for several stiffened constructions in compression based on wide-column and local instability considerations. (An applicable construction is shown in Fig. 1-1). These are discussed in Appendix B and are supplemented therein with analyses of other types of construction.

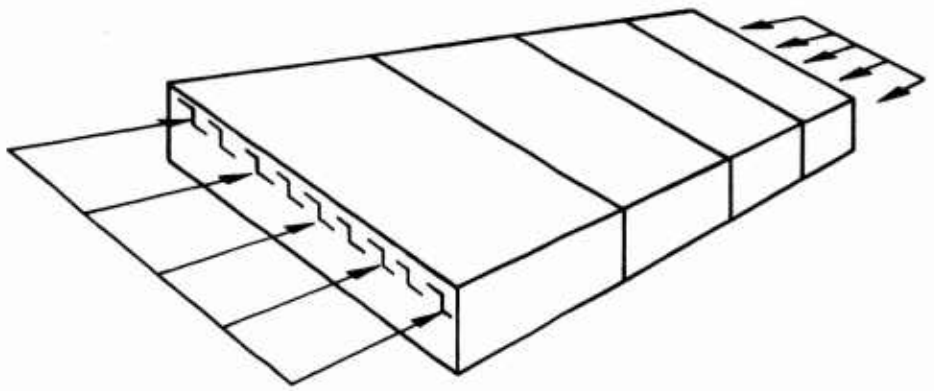

Fig. 1-1 Multi-Rib Wing Box Construction

However, there are many applications in which wide-column analysis is too conservative. Such cases are illustrated in Figs. 1-2a and 1-2b. It is emphasized that, for

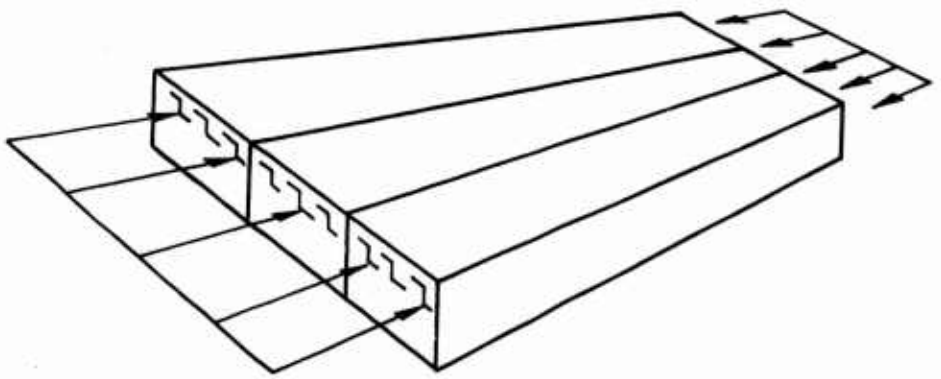

Fig. 1-2a Multi-Spar Wing Box Construction

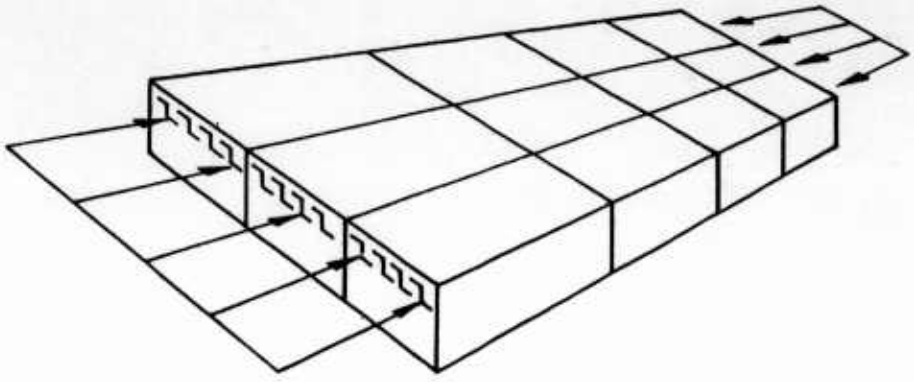

Fig. 1-2b Rib-Spar Wing Box Construction

minimum weight, these applications should not be analyzed as wide columns but as stiffened panels with support along the unloaded edges. It is the minimum weight analysis of this class of panels that is considered in the body of this report.

The development of the equations leading to the determination of minimum weight geometries for each of the four listed types of construction is similar. Only minor modifications in approach, from one to another, are necessary. Therefore, equations are developed for the zee-stiffened panel construction alone. For the remaining constructions, only the final equations are presented.

The method of minimum weight analysis is essentially that used by Zahorski (Ref. 1), Shanley (Ref. 2), and Crawford, Burns and Tilcens (Ref. 3), as well as some others. Minimum weight results when the structure is proportioned in such manner that both general and local instability become critical under the applied loading. As in previous analyses of this type the necessary simplifying assumption is made that there is no coupling among the various modes of instability. Following the analyses, there is a comparison of the relative efficiencies of the constructions considered.

Section 2

MINIMUM WEIGHT ANALYSES

2.1 ANALYSIS OF ZEE-STIFFENED FLAT PANELS IN COMPRESSION

In this first analysis, the minimum weight of zee-stiffened panels uniformly compressed in the direction of the stiffening elements is determined. Equations for calculating the critical stresses for both local and general modes of instability are available in Ref. 4. When these equations are suitably combined, the following general form may be obtained.

Loading-Material Index = Efficiency Factor X Weight Index

For some panel constructions, the efficiency factor is found to be independent of the other variables above. To find the minimum weight in these cases, the problem resolves into finding the maximum value of the efficiency factor; i.e., the efficiency factor, which is a function of the panel geometric parameters, is maximized. Such a solution indicates that a panel configuration whose proportions remain constant is the minimum weight design. This may be expressed mathematically in the form:

$$\frac{N_x}{b \cdot \bar{\eta} E} = \mathcal{E}\left(\frac{\bar{t}}{b}\right)^m \qquad (2.1)$$

Here, N_x is the applied load per inch of panel, b is the overall width of panel, $\bar{t}$ is the equivalent flat plate thickness of the stiffened panel (equal to the cross-sectional area of the panel divided by b), $\bar{\eta}$ is the effective plasticity reduction factor, and m is an exponent related to the particular geometry. A chart which is supplementary to the minimum weight equation is presented, which shows the relationship between $\mathcal{E}$ and panel geometry. This provides the designer with a view of the relative efficiency of an existing design on the basis of comparison with the minimum weight

design. It is seen that the panel proportions remaining constant, as noted above, involve ratios of widths and/or thicknesses alone; proportions involving both width and thickness, such as t/b, are proportional to the loading intensity and vary accordingly.

There are a number of panel constructions, including the zee-stiffened panel, in which the efficiency factor is related to the magnitude of the load. Consequently, the design proportions which provide minimum weight at one load level are not the same as those which provide minimum weight at some other load level. These constructions must be investigated over the entire practical load range, and the end result is a minimum-weight design "envelope" which is presented as a function of $N_x/b\bar{\eta}E$ and $\bar{t}/b$, and identifies the areas where associated geometric proportions yield minimum weight. A supplementary chart is presented for these cases as a source of additional information to define the minimum-weight designs, and also to relate less efficient panel geometries to the optimum. The minimum-weight design envelope can be expressed approximately as a simple relationship between $\bar{t}/b$ and $N_x/b\bar{\eta}E$ which may be represented mathematically in the form of Eq. (2.1). This is helpful in establishing the relative efficiencies of various panel constructions in preliminary design work.

Occasionally it may be demonstrated that the interrelation of efficiency factor and load magnitude as discussed above is small enough to be neglected. The minimum weight design may then be expressed in the form of Eq. (2.1), and efficiency may be assumed to be a function of geometric proportions alone as initially discussed. An example of this type of solution is the minimum weight analysis for truss-core, semi-sandwich panels. (Subsection 2.3).

2.1.1 Derivation of Equations

The geometry of a zee-stiffened panel is given in Fig. 2-1:

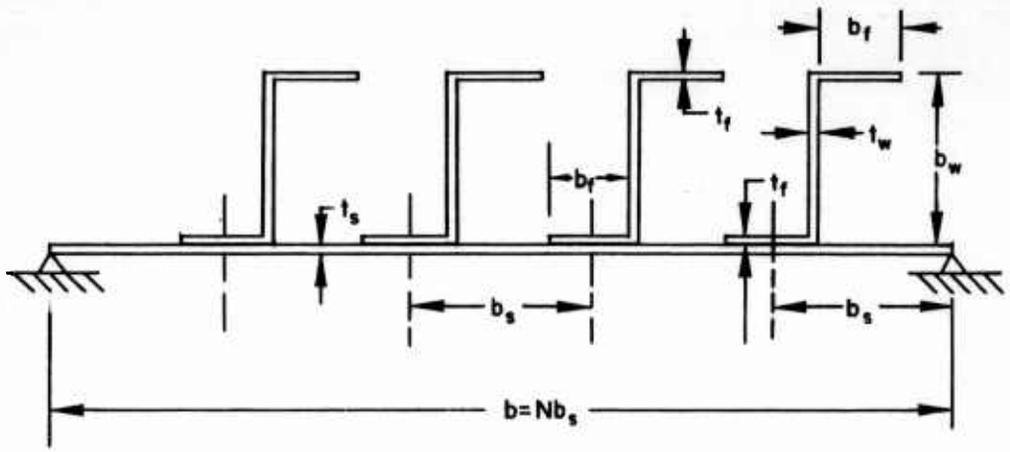

Fig. 2-1 Cross-Sectional Geometry of a Zee-Stiffened Panel

In order to simplify the minimum weight analysis, certain general assumptions are made, as follows:

(1) All sides of the composite panel are simply supported.

(2) The intersecting edges of all elements composing the stiffened panel are simply supported.

(3) The aspect ratio of the composite panel, as well as its elemental panels, is sufficiently large to be considered infinite.

(4) Orthotropic plate theory may be used as the basis of the analysis for the general mode of instability (according to Ref. 4, this is a good assumption as long as the stiffeners number more than two).

Assumption (2) may be either conservative or unconservative, as stated in Ref. 4, but may be generally considered conservative for minimum weight designs in which the skin and stiffener critical stresses are approximately the same.

In the interest of simplicity it is advantageous to minimize the number of geometric variables involved while preserving the practical application of the end results. Consequently, the following additional specific assumptions are made:

(5) The free and attached flanges of the zee stiffener are of equal length and thickness.

(6) The half-thickness of the skin is neglibible in comparison to the zee web height, b_w.

(7) The thickness of the zee flanges is equal to the thickness of the zee web, $t_f = t_w$.

As a result of assumptions (5) and (6), $\bar{z}$, the distance from the midsurface of the skin to the stiffener centroidal axis, is equal to $b_w/2$.

Assumptions (2) and (3) permit certain geometric relationships to be defined. Since the outstanding flange of the zee stiffener has been assumed to be long and simply supported at the web of the zee, K_F for local instability is 0.5 according to Ref. 4. Likewise, $K_w = 4.0$ for local instability of the web of the stiffener and $K_S = 4.0$ for local instability of the panels between the stiffeners.

The local instability equations for each of these elements can be written as follows:

$$\sigma_{cr_{L_f}} = \eta_L \frac{E\pi^2}{12(1-\mu^2)} \left(\frac{t_f}{b_f}\right)^2 K_F \qquad (2.2)$$

$$\sigma_{cr_{L_w}} = \eta_L \frac{E\pi^2}{12(1-\mu^2)} \left(\frac{t_w}{b_w}\right)^2 K_W \qquad (2.3)$$

$$\sigma_{cr_{L_s}} = \eta_L \frac{E\pi^2}{12(1-\mu^2)} \left(\frac{t_s}{b_s}\right)^2 K_S \qquad (2.4)$$

Taking $t_f = t_w$, assumption (7), and substituting the above values for K_F, K_W and K_S, the following geometric proportions result when all the elements buckle at the same stress:

$$\frac{b_f}{b_w} = 0.3535 \tag{2.5}$$

$$\frac{t_w}{t_s} = \frac{b_w}{b_s} \tag{2.6}$$

The approximation that K_S is equal to 4.0 is substantiated by referring to Fig. 2.2-10 of Ref. 4, which shows the buckling coefficient, K_S, for a plate having zee-section integral stiffeners. Values of K_S coinciding with the requirements of Eqs. (2.5) and (2.6) are very nearly 4.0 in Fig. 2.2-10 as well as in each of the three other groups of curves presented. Thus, two geometric parameters may be eliminated from the ensuing derivation, b_f/b_w and either b_w/b_s or t_w/t_s.

The equations for the local instability of the skin and general instability of the composite panel as taken from Ref. 4, are:

$$\sigma_{cr_L} = \eta_L \frac{E\pi^2}{12(1-\mu^2)} \left(\frac{t_s}{b_s}\right)^2 K_S \tag{2.7}$$

$$\sigma_{cr_G} = \eta_G \frac{E\pi^2}{12(1-\mu^2)} \left(\frac{t_s}{b_s}\right)^2 K_G \tag{2.8}$$

For optimum design, both modes of instability become critical under the applied loading N_x. Therefore,

$$\sigma_{cr_L} = \sigma_{cr_G} = N_x/\bar{t} = \sigma \tag{2.9}$$

Combining Eqs. (2.7), (2.8) and (2.9);

$$N_x/b\bar{\eta}E = \frac{\pi^2}{12(1-\mu^2)}\left(\frac{t_s}{b_s}\right)^2 \sqrt{K_S}\,\sqrt{K_G}\,\left(\frac{\bar{t}}{b}\right) \qquad (2.10)$$

The quantity $\bar{\eta}$ represents an effective plasticity reduction factor:

$$\bar{\eta} = \sqrt{\eta_L\,\eta_G}$$

The value of η_L to be used in this analysis is taken from Ref. 4:

$$\eta_L = \sqrt{\eta_T}$$

while η_G is taken equal to η_T. Thus, in this analysis:

$$\bar{\eta} = \left[\eta_T\right]^{3/4}$$

The buckling coefficient for general instability (Ref. 4) may be expressed as follows:

$$K_G = \frac{2\left\{\left[1 + \frac{N-1}{N}\left(\frac{EI}{b_s D}\right)\left(1 + \frac{\frac{A\bar{z}^2}{I}}{1 + \frac{0.88A}{b_s t_s}}\right)\right]^{1/2} + 1\right\}}{N^2\left[\frac{N-1}{N}\left(\frac{A}{b_s t_s} + 1\right)\right]} \qquad (2.11)$$

Before proceeding further, some of the quantities appearing in Eqs. (2.10) and (2.11) are evaluated, making use of Eqs. (2.5) and (2.6). For definition of these quantities, refer to the nomenclature.

$$\bar{t}/b = \frac{t_s}{b_s}\frac{1}{N}\left[1 + 1.707\,\frac{N-1}{N}\left(\frac{b_w}{b_s}\right)^2\right] \tag{2.12}$$

$$D = \frac{Et_s^3}{12(1-\mu^2)} \tag{2.13}$$

$$A = 1.707\,t_w b_w \tag{2.14}$$

$$I = \frac{t_w}{12}b_w^3 + 2(t_f b_f)\left(\frac{b_w}{2}\right)^2 + \frac{1}{6}b_f t_f^3 \tag{2.15}$$

The last term will be assumed negligible in comparison to the first two terms. Therefore:

$$I = 0.260\,t_w b_w^3 \tag{2.16}$$

$$\frac{A}{b_s t_s} = 1.707\left(\frac{b_w}{b_s}\right)^2 \tag{2.17}$$

$$\frac{EI}{b_s D} = \frac{3.12(1-\mu^2)\left(\frac{b_w}{b_s}\right)^4\left[1 + 1.707\,\frac{N-1}{N}\left(\frac{b_w}{b_s}\right)^2\right]^2}{(\bar{t}/b)^2\,N^2} \tag{2.18}$$

$$\frac{\frac{A\bar{z}^2}{I}}{1 + \frac{0.88A}{b_s t_s}} = \frac{1.641}{1 + 1.502\left(\frac{b_w}{b_s}\right)^2} \tag{2.19}$$

Substitutions in Eq. (2.10) from the above equations are made, assuming $\mu = 0.3$. For convenience, $\sqrt{K_G}$ is expressed separately.

$$\frac{N_x}{b \cdot \bar{\eta} E} = \frac{1.8076\ N^2 \sqrt{K_G}}{\left[1 + 1.707\ \frac{N-1}{N}\left(\frac{b_w}{b_s}\right)^2\right]^2} \left(\frac{\bar{t}}{b}\right)^3 \tag{2.20}$$

$$\sqrt{K_G} = \sqrt{\frac{2\left\{\left[1 + \frac{2.839\ \frac{N-1}{N}\left(\frac{b_w}{b_s}\right)^4 \left[1 + 1.707\ \frac{N-1}{N}\left(\frac{b_w}{b_s}\right)^2\right]^2}{(\bar{t}/b)^2 \cdot N^2}\left(1 + \frac{1.641}{\left[1 + 1.502\left(\frac{b_w}{b_s}\right)^2\right]}\right)\right]^{1/2} + 1\right\}}{N^2\left[1 + 1.707\ \frac{N-1}{N}\left(\frac{b_w}{b_s}\right)^2\right]}} \tag{2.21}$$

Equation (2.20) would be of the form of Eq. (2.1) if $\sqrt{K_G}$, Eq. (2.21), did not contain an unfactorable function of $\bar{t}/b$; however, it will be seen later that in the range of interest, Eq. (2.20) can be expressed approximately in the form of Eq. (2.1). Since minimum weight results when both general and local instability become critical under the applied load, both K_L and K_G are set equal to 4.0 in Eqs. (2.20) and (2.21). Thus,

$$\frac{N_x}{b\bar{\eta}E} = \frac{3.615\ N^2}{\left[1 + 1.707\ \frac{N-1}{N}\left(\frac{b_w}{b_s}\right)^2\right]} \left(\frac{\bar{t}}{b}\right)^3 \tag{2.22}$$

$$\frac{\bar{t}}{b} = \sqrt{\frac{2.839\,\frac{N-1}{N}\left(\frac{b_w}{b_s}\right)^4\left[1 + 1.707\,\frac{N-1}{N}\left(\frac{b_w}{b_s}\right)^2\right]^2\left[1 + \frac{1.641}{1 + 1.502\left(\frac{b_w}{b_s}\right)^2}\right]}{N^2\left\{\left[2N^2\left[1 + 1.707\,\frac{N-1}{N}\left(\frac{b_w}{b_s}\right)^2\right] - 1\right]^2 - 1\right\}}} \qquad (2.23)$$

The procedure for determining minimum weight geometric proportions from Eqs. (2.22) and (2.23) is as follows:

(1) Select a value of N

(2) Select a range of b_w/b_s values

(3) Calculate $(\bar{t}/b)$'s from Eq. (2.23) for the assumed range of b_w/b_s values.

(4) Calculate $N_x/b \cdot \bar{\eta}\, E$ from Eq. (2.22) for the range of compatible $\bar{t}/b$ and b_w/b_s values.

(5) Repeat steps (1) through (4) for sufficient N values to determine the minimum weight design envelope over the practical range of $N_x/b \cdot \bar{\eta}\, E$.

Equations (2.22) and (2.23) are applicable as long as $N > 3$, according to assumption (4). The following analysis is used in conjunction with Eq. (2.22) when N is equal to 2 or 3.

The special cases of one and two stiffener panels were considered in Ref. 5, and are analyzed with the assistance of a design chart which is reproduced in Ref. 4 as Fig. 2.2-2. This chart gives a plot of K_G versus

$$\frac{EI}{b_s D}\left[1 + \frac{A\bar{z}^2/I}{1 + \frac{Z_{nq}\,A}{b_s t_s}}\right]$$

for various values of $A/b_s t_s$. The expression $A/b_s t_s$ is presented in terms of b_w/b_s in Eq. (2.17). Employing Eqs. (2.17), (2.18), (2.19), it is found that:

$$\frac{EI}{b_s D}\left[\frac{1 + \frac{A\bar{z}^2}{I}}{1 + \frac{Z_{nq} A}{b_s t_s}}\right]$$

$$= \frac{2.839\left(\frac{b_w}{b_s}\right)^4\left[1 + 1.707\,\frac{N-1}{N}\left(\frac{b_w}{b_s}\right)^2\right]^2}{(\bar{t}/b)^2\, N^2}\left[1 + \frac{1.641}{1 + 1.707\, Z_{nq}\left(\frac{b_w}{b_s}\right)^2}\right] \qquad (2.24)$$

Using the same reasoning as was applied in obtaining a solution to Eqs. (2.20) and (2.21), minimum weight designs for these special cases are determined by the following procedure.

(1) Select N equal to either 2 (1 stiffener) or 3 (2 stiffeners).

(2) Select a range of b_w/b_s values.

(3) Taking $K_G = 4.0$, determine from Fig. 2.2-2 of Ref. 4 the proper values of the abscissa. Set these values equal to the right-hand side of Eq. (2.24) and solve for $(\bar{t}/b)$'s corresponding to the range of b_w/b_s values.

(4) Calculate $N_x/b \cdot \bar{\eta} E$ from Eq. (2.22) for the range of compatible $\bar{t}/b$ b_w/b_s values.

2.1.2 Minimum Weight Envelope and Auxiliary Chart

The above analysis has been presented in nondimensional form, and is applicable to all materials. In order that a graphical presentation of this analysis shall include the majority of the designs of interest, the expected maximum and minimum values

of $\bar{t}/b$ and $N_x/b \cdot \bar{\eta} E$ for a number of materials have been determined, with the result that the following practical ranges of these parameters are established:

$$10^{-4} < \bar{t}/b < 10^{-1}$$

$$10^{-9} < N_x/b\bar{\eta}E < 10^{-2}$$

It may be reasoned that when $\bar{t}/b \approx 10^{-1}$, the design approaches proportions where stability is no longer a problem and a flat plate is the most economical construction. The range of $\bar{t}/b > 10^{-1}$, therefore, is probably not significant in actual design. (Section 4 gives comparisons of zee-stiffened panel efficiency and unstiffened panel efficiency in this $\bar{t}/b$ range).

Equations (2.22) and (2.23) have been solved for a large number of combinations of N and b_w/b_s, and these solutions are presented in Figs. 2-2a and 2-2b over the above ranges of $\bar{t}/b$ and $N_x/b \cdot \bar{\eta} E$. It is noted from these figures that the number of stiffeners for minimum weight design varies with the magnitude of the load, as previously shown. Further, the equation of the minimum weight envelope over the range of $N_x/b \cdot \bar{\eta}E$ from 10^{-9} to 10^{-4} is approximately

$$\frac{N_x}{b\bar{\eta}E} = 1.030 \left(\frac{\bar{t}}{b}\right)^{2.36} \qquad (2.25)$$

An auxiliary chart is presented (Fig. 2-3) to show the relation between $\bar{t}/b$ and b_w/b_s for a given value of N, and also to show the relation between the most efficient geometries and less efficient geometries. Note the relatively narrow range of optimum b_w/b_s values. Since N = 2 is the smallest value of N for a zee-stiffened panel, it is the most efficient design for any $N_x/b\bar{\eta}E$ value above 10^{-4}. Therefore, there is no upper limit on the optimum value of b_w/b_s for this case. Any value of b_w/b_s necessary to support a given $N_x/b\bar{\eta}E$ above 10^{-4} is optimum. The following

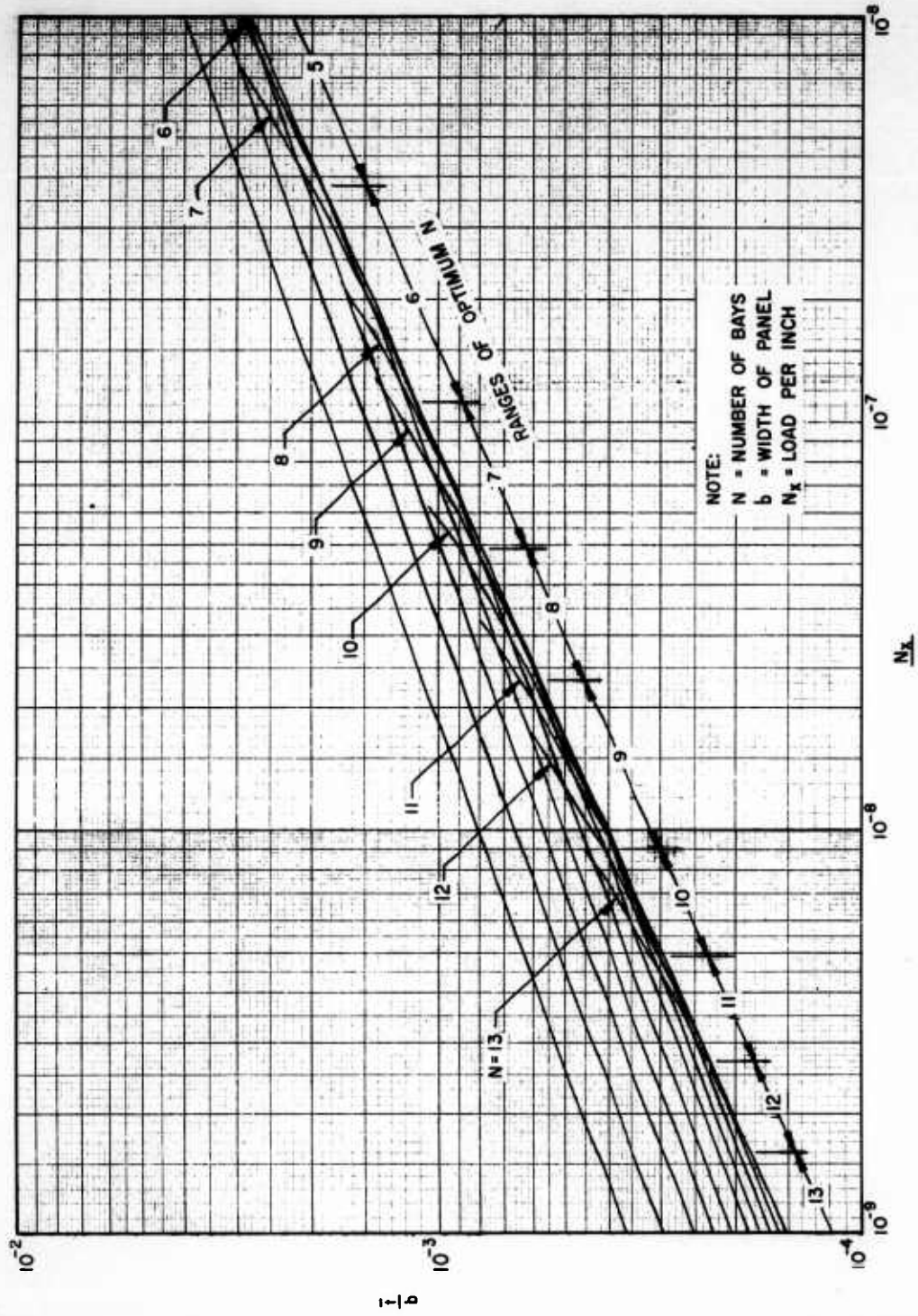

Fig. 2-2a Efficiency Chart for Zee-Stiffened Flat Panels in Compression (Stiffeners Parallel to Load)

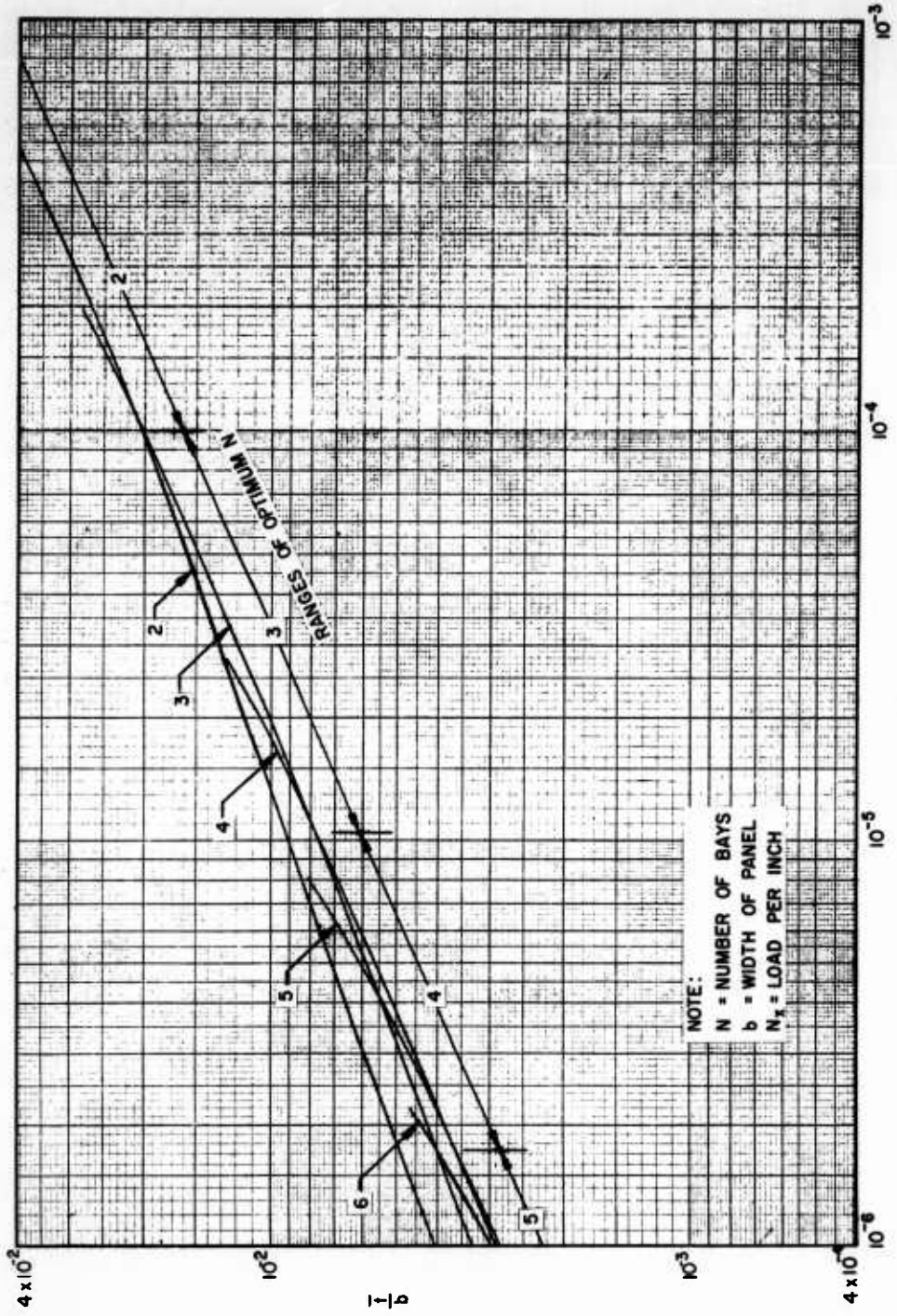

Fig. 2-2b Efficiency Chart for Zee-Stiffened Flat Panels in Compression (Stiffeners Parallel to Load) (Continuation of Fig. 2-2a)

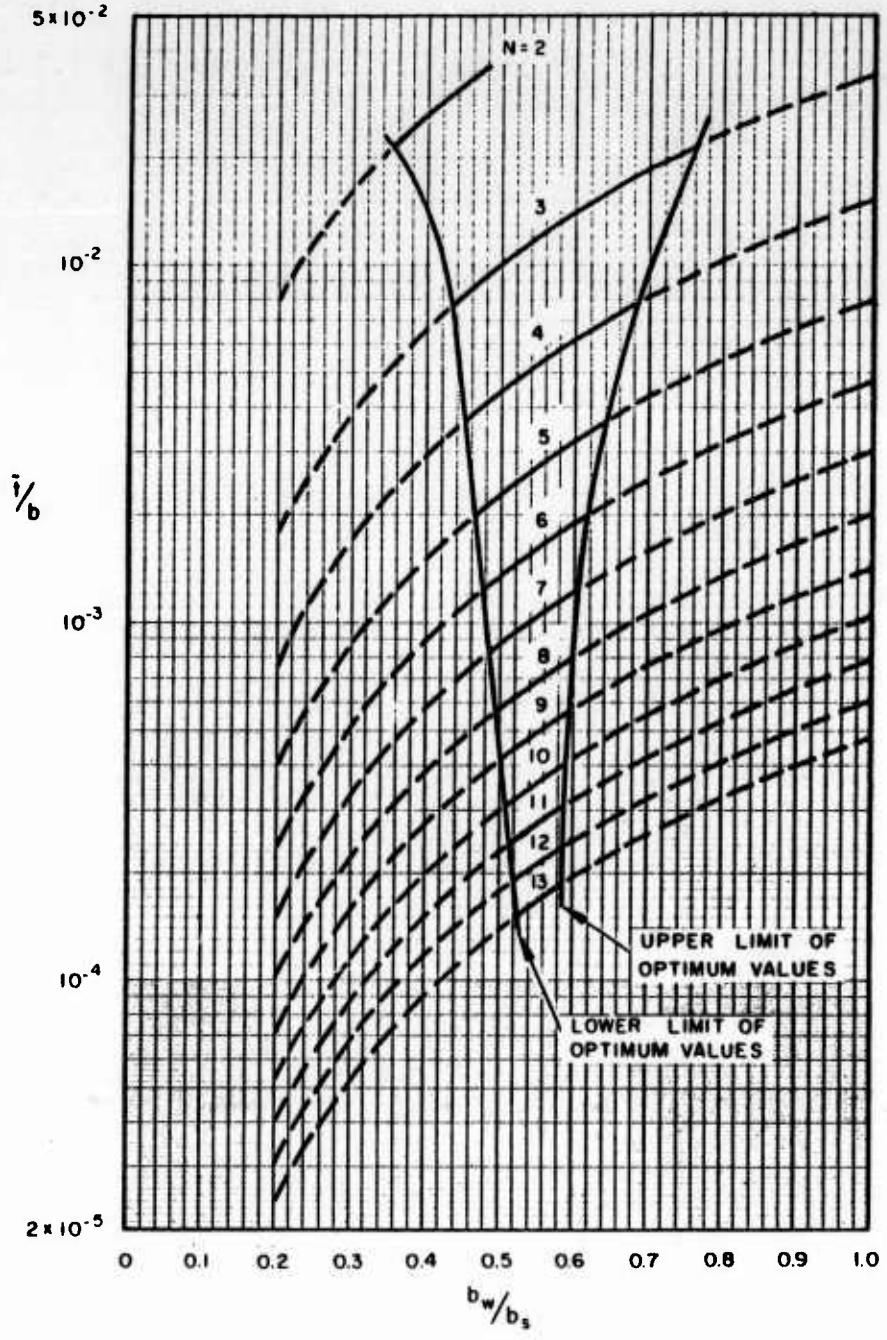

Fig. 2-3 Auxiliary Design Chart for Zee-Stiffened Flat Panels in Compression

equations are necessary in conjunction with Figs. 2-2a, 2-2b and 2-3 to determine minimum weight proportions:

$$b_s = b/N \tag{2.26}$$

$$t_s = \frac{b_s \cdot \frac{\bar{t}}{b} \cdot N}{1 + 1.707 \frac{N-1}{N}\left(\frac{b_w}{b_s}\right)^2} \tag{2.27}$$

$$t_w = t_f = t_s\left(\frac{b_w}{b_s}\right) \tag{2.28}$$

$$b_f = 0.3535\, b_w \tag{2.29}$$

Usually, the first step in finding a minimum weight design is solving for $N_x/b\bar{\eta}E$. Because of the presence of the effective plasticity factor in this parameter, its effect must be considered when designing in the plastic stress region where $\bar{\eta} < 1$. Two methods for evaluating $\bar{\eta}$ shall now be discussed.

If $\bar{\eta}$ is taken as $\left[\eta_T\right]^{3/4}$ as recommended previously, $N_x/b\bar{\eta}E$ assumes the following form when the Ramberg-Osgood formulation for E_T (Ref. 6) is substituted:

$$\frac{N_x}{b\bar{\eta}E} = \frac{N_x}{bE}\left[1 + \frac{3}{7}n\left(\frac{N_x}{\bar{t} \cdot F_{0.7}}\right)^{n-1}\right]^{3/4} \tag{2.30}$$

The seven-tenths secant yield stress, $F_{0.7}$, and the shape factor defining the knee of the compressive stress-strain curve, n, are material properties which are presented in several references (see Ref. 7). They may also be calculated directly, using

the methods presented in Ref. 8. Thus, defining the true value of $N_x/b\bar{\eta}E$ resolves into a trial and error procedure:

(1) Calculate $N_x/b\bar{\eta}E$ where $\bar{\eta} = 1$

(2) Determine $\bar{t}/b$ from Fig. 2-2a or 2-2b

(3) Having values of $F_{0.7}$ and n at hand, substitute $\bar{t}$ into the right hand side of Eq. (2.30) and evaluate the expression.

(4) If the right-hand side of Eq. (2.30) does not equal the left-hand side, adjust $N_x/b\bar{\eta}E$ accordingly (assign $\bar{\eta}$ a value less than one) and repeat steps (1) through (3), above, until the right and left hand sides of the equation are equal. The resulting value of $N_x/b\bar{\eta}E$ is the true value at some plastic stress. If steps (1) through (3) produce an equality on the first test, the applied stress is, of course, elastic.

The second method is primarily of assistance when many minimum weight designs are desired in a particular material in a given thermal environment. Taking $\bar{\eta} = \left[\eta_T\right]^{3/4}$ a chart of $\sigma/\bar{\eta}$ versus σ is drawn (Fig. 2-4) representing the desired material and the thermal environment.

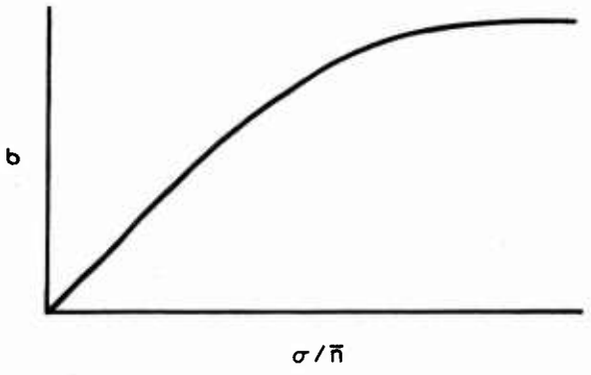

Fig. 2-4 Typical Example of the Variation of $\sigma/\bar{\eta}$ with σ

The following procedure is then used:

(1) From Eq. (2.25) it can be seen that for minimum weight geometries:

$$\frac{N_x/b\bar{\eta}E}{\bar{t}/b} = \frac{\sigma}{\bar{\eta}E} = 1.030\left(\frac{\bar{t}}{b}\right)^{1.36}$$

from which $\sigma/\bar{\eta}$ values may be determined over a range of $\bar{t}/b$ values.

(2) Utilizing a chart of the type of Fig. 2-4, find σ for each value of $\sigma/\bar{\eta}$ determined in (1).

(3) Solve for N_x/b by multiplying σ by $\bar{t}/b$.

(4) Plot $\bar{t}/b$ vs N_x/b. This chart includes the effects of $\bar{\eta}$. The value of $\bar{t}/b$ found by entering the chart with an N_x/b is the optimum value. The dimensions of the design may then be found, with the help of Fig. 2-3.

Two example problems are presented below to illustrate the use of the charts.

Problem 1

Given a bay 20 inches wide with simply supported edges which appears in a structure similar to Fig. 1-2b.

Determine the minimum weight, flat, longitudinally zee-stiffened, all beta titanium panel design to carry a longitudinally applied load of 300,000 pounds at room temperature.

Material Data (Ref. 5)

$$F_{0.7} = 198{,}000 \text{ psi}$$

$$n = 22$$

$$E = 16{,}500{,}000 \text{ psi}$$

(1) Determine $N_x/b\bar{\eta}E$, taking $N_x/b = \frac{P}{b^2} = \frac{300,000}{(20)^2} = 750$. The first method previously described for evaluating $\bar{\eta}$ will be used.

a. $$N_x/b\bar{\eta}E = \frac{750}{16,500,000} = 4.55 \times 10^{-5}$$

b. From Fig. 2-2a, 2-2b, $\bar{t}/b = 1.43 \times 10^{-2}$, $N = 3$.

c. Substituting into the right hand side of Eq. (2.30):

$$4.55 \times 10^{-5} \left| \begin{array}{l} 4.55 \times 10^{-5} \left[1 + \frac{3}{7} (22) \left(\frac{750}{1.43 \times 10^{-2} (198,000)} \right)^{21} \right]^{3/4} \\ \\ 4.55 \times 10^{-5} \ (1.0000) \end{array} \right.$$

$$4.55 \times 10^{-5} = 4.55 \times 10^{-5}$$

The true value of $N_x/b\bar{\eta}E = 4.55 \times 10^{-5}$ (and $\bar{t}/b = 1.43 \times 10^{-2}$, $\bar{t} = 0.286$, $N = 3$).

(2) From Fig. 2-3, $b_w/b_s = 0.61$. Equations (2.26) through (2.29) yield:

$$b_s = \frac{20}{3} = 6.67 \text{ inches}$$

$$b_w = 0.61\,(6.67) = 4.07 \text{ inches}$$

$$t_s = \frac{6.67\,(1.43 \times 10^{-2})3}{1 + 1.707\,(2/3)\,(0.61^2)} = 0.201 \text{ inch}$$

$$t_w = t_f = 0.201\,(0.61) = 0.1225 \text{ inch}$$

$$b_f = 0.3535\,(4.07) = 1.44 \text{ inches}$$

The thicknesses found in step (2), above, not being standard gages, must usually be made into standard gages, preferably in such a manner that a minimum practical weight results. The following procedure is recommended.

Since the minimum $\bar{t}/b$ calculated above represents the minimum theoretical weight, it follows that any $\bar{t}/b$ based on standard gages will be higher. If a horizontal line is drawn on Fig. 2-3 at $(\bar{t}/b)_{min}$, any non-minimum $\bar{t}/b$ will be above this line, and may be associated with an N either larger or smaller than the N corresponding to $(\bar{t}/b)_{min}$, the selection depending on the magnitude of b_w/b_s. It is assumed that t_w, t_s and N for minimum practical weight are in the same range as t_w, t_s and N for minimum theoretical weight. Thus, one of the four following designs possesses minimum practical weight. The upward arrow signifies raising the thicknesses to the next standard gage, the downward arrow the converse.

Trial	1*	2	3	4
t_w	↑	↑	↑	↓
t_s	↑	↑	↓	↑

*In Trial 1, b_w, b_s and N remain the theoretically optimum values. In the remaining trials, $t_w/t_s = b_w/b_s$.

With the exception of Trial 1, the allowable N_x is found for all trials by a procedure which is the reverse of that shown in the example problem. The combination to carry

the applied N_x having the lowest $\bar{t}/b$ is the minimum practical weight. In the case of Trial 1, it is assumed that the addition of weight without altering b_w, b_s, or N increases the load-carrying ability of the stiffened plate. Further, unless $t_w/t_s = b_w/b_s$ the design charts are invalid. In this single instance:

$$\left[\bar{t}/b\right]_{\text{Trial \#1}} = \frac{t_s}{b_s}\,\frac{1}{N}\left[1 + 1.707\,\frac{N-1}{N}\left(\frac{t_w}{t_s}\right)\left(\frac{b_w}{b_s}\right)\right]$$

Problem 2

This problem is intended to illustrate that the minimum weight design charts may be used for stress analysis as well as for design, shown in Prob. 1. This usage is made possible by the inclusion of additional, non-optimum information in the minimum weight design charts.

Given a simply-supported panel, 12-inches wide and stiffened with equally-spaced zee-stiffeners, as shown in the following sketch.

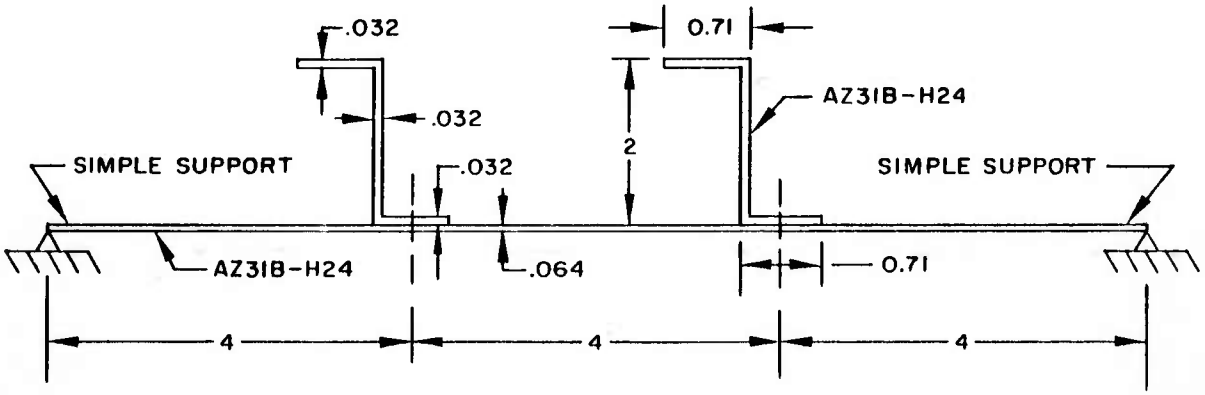

Determine how this design compares with the minimum weight design for carrying a load of 20,000 pounds parallel to the stiffeners. The load is applied at room temperature.

Material Data (Ref. 5)

$$F_{0.7} = 27{,}000 \text{ psi}$$

$$n = 6$$

$$E = 6{,}500{,}000 \text{ psi}$$

(1) From the sketch, $b_w/b_s = 0.5$, $N = 3$. Referring to Fig. 2-3, it is noted that these parameters fall in the optimum range. Thus, the design is proportioned to carry some particular load at minimum weight. Points in the dashed areas of Fig. 2-3 indicate less efficient designs.

(2) Check the load-carrying ability of this design. From Fig. 2-3, $\bar{t}/b = 10^{-2}$. From Fig 2-2a, 2-2b, $N_x/b\bar{\eta}E = 1.95 \times 10^{-5}$. The value of N_x, denoted N_{x_1}, representing a value of $N_x/b\bar{\eta}E$ of 1.95×10^{-5} (using the same methods as in Prob. 1), is 1485 lb/in (here $\bar{\eta} < 1$). But $N_{x_{applied}}$ is $20{,}000/12 = 1667$ lb/in. The design is therefore understrength.

(3) The minimum weight design to carry the load may be determined from steps similar to those in Prob. 1, which result in the following quantities:

$$N_x/b\bar{\eta}E = 2.25 \times 10^{-5}$$

$$\bar{t}/b = 1.06 \times 10^{-2}$$

$$N = 3$$

$$\bar{t} = 0.127 \text{ inch}$$

$$b_w/b_s = 0.52$$

$$b_s = 4 \text{ inches}$$

$$b_w = 2.08 \text{ inches}$$

$$t_s = 0.0973 \text{ inch}$$

$$t_w = t_f = 0.0506 \text{ inch}$$

$$b_f = 0.735 \text{ inch}$$

Comparing these dimensions with those on the sketch above, note that the primary adjustments are in t_s and t_w. If in step (2) above, $N_{x_{applied}} \leq N_{x_1}$, quite different conclusions would have been drawn. An equality signifies the design is a minimum weight design; when $N_{x_{applied}} < N_{x_1}$ the design is safe and has a positive margin of safety, as follows:

$$M.S. = \frac{N_{x_1}}{N_{x_{applied}}} - 1 \qquad (2.31)$$

If the margin of safety indicated by Eq. (2.31) is sizable, it is desirable to perform calculations similar to those in Prob. 1 to minimize the margin and thereby lighten the design. The discussion following Prob. 1, relating to the selection of standard gages for minimum practical weight, is applicable here also.

2.2 ANALYSIS OF UNFLANGED, INTEGRALLY-STIFFENED FLAT PANELS

The geometry of this construction is shown in Fig. 2-5. Many of the assumptions made for zee-stiffened panels may be applied here, owing to the similarity of the two constructions. For example, general assumptions (1) through (4) (p. 2-3) are employed. Also, it is assumed that $\bar{z} = b_w/2$, $\mu = 0.3$.

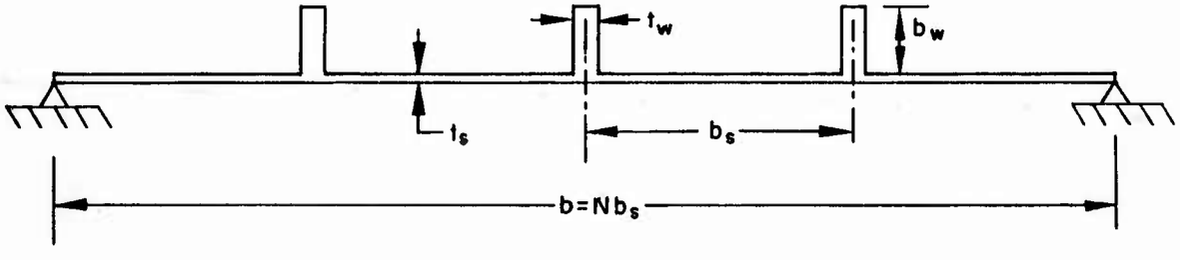

Fig. 2-5 Cross-Sectional Geometry of an Unflanged Integrally-Stiffened Panel

The effect of general assumptions (1) and (2) on this construction may be determined by referring to Eqs. (2.3) and (2.4) and taking $K_W = 0.5$ and $K_S = 4.0$. Thus,

$$\frac{t_w}{t_s} = 2\sqrt{2}\,\frac{b_w}{b_s} \tag{2.32}$$

The derivation using the above assumptions yields:

$$\frac{\bar{t}}{b} = \sqrt{\frac{10.294\left[\frac{N-1}{N}\left(\frac{b_w}{b_s}\right)^2\right]^2\left\{1 + 3.535\,\frac{N-1}{N}\left(\frac{b_w}{b_s}\right)^2 + 2\left[\frac{N-1}{N}\left(\frac{b_w}{b_s}\right)^2\right]^2\right\}}{N(N-1)\left\{\left[2N^2\left(1 + 2.828\,\frac{N-1}{N}\left[\frac{b_w}{b_s}\right]^2\right) - 1\right]^2 - 1\right\}}} \tag{2.33}$$

$$\frac{N_x}{b\bar{\eta}E} = \frac{3.615\,N^2}{\left[1 + 2.828\,\frac{N-1}{N}\left(\frac{b_w}{b_s}\right)^2\right]^2}\left(\frac{\bar{t}}{b}\right)^3 \tag{2.34}$$

where $\bar{\eta}$ is taken equal to $\left[\eta_T\right]^{3/4}$, the same as in the case of zee-stiffened panels.

Note that these equations are similar in form to Eqs. (2.22) and (2.23), and were formulated with the same line of reasoning. When $N \leq 3$, that is, when orthotropic plate theory is not acceptable for the analysis of the general mode of instability, the

same procedure is followed as outlined previously in this section. For this case:

$$\frac{EI}{b_s D} = \left[1 + \frac{\frac{A\bar{z}^2}{I}}{1 + \frac{Z_{nq} A}{b_s t_s}} \right] = \frac{2.573 \left(\frac{b_w}{b_s}\right)^4 \left[1 + 2.828 \frac{N-1}{N} \left(\frac{b_w}{b_s}\right)^2 \right]^2}{\left(\frac{\bar{t}}{b}\right)^2 N^2}$$

$$- \left[1 + \frac{3}{1 + 2.828 Z_{nq} \left(\frac{b_w}{b_s}\right)^2} \right] \qquad (2.35)$$

Solutions to equations (2.33) and (2.34) are presented in Figs. 2-6a, 2-6b, and 2-7. Figure 2-6a, 2-6b shows the minimum weight envelope, which may be mathematically expressed by Eq. (2.36) over the range of $N_x/b\bar{\eta}E$ from 10^{-9} to 10^{-4} as

$$\frac{N_x}{b\bar{\eta}E} = 0.970 \left(\frac{\bar{t}}{b}\right)^{2.38} \qquad (2.36)$$

Figure 2-7 indicates the optimum combinations of b_w/b_s and N, and also defines non-optimum combinations. The following equations are used in connection with Figs. 2-6a, 2-6b, and 2-7 for design purposes:

$$b_s = \frac{b}{N} \qquad (2.26)$$

$$t_s = \frac{b_s \left(\frac{\bar{t}}{b}\right) N}{1 + 2.828 \frac{N-1}{N} \left(\frac{b_w}{b_s}\right)^2} \qquad (2.37)$$

$$t_w = 2.828 \, t_s \left(\frac{b_w}{b_s}\right) \qquad (2.38)$$

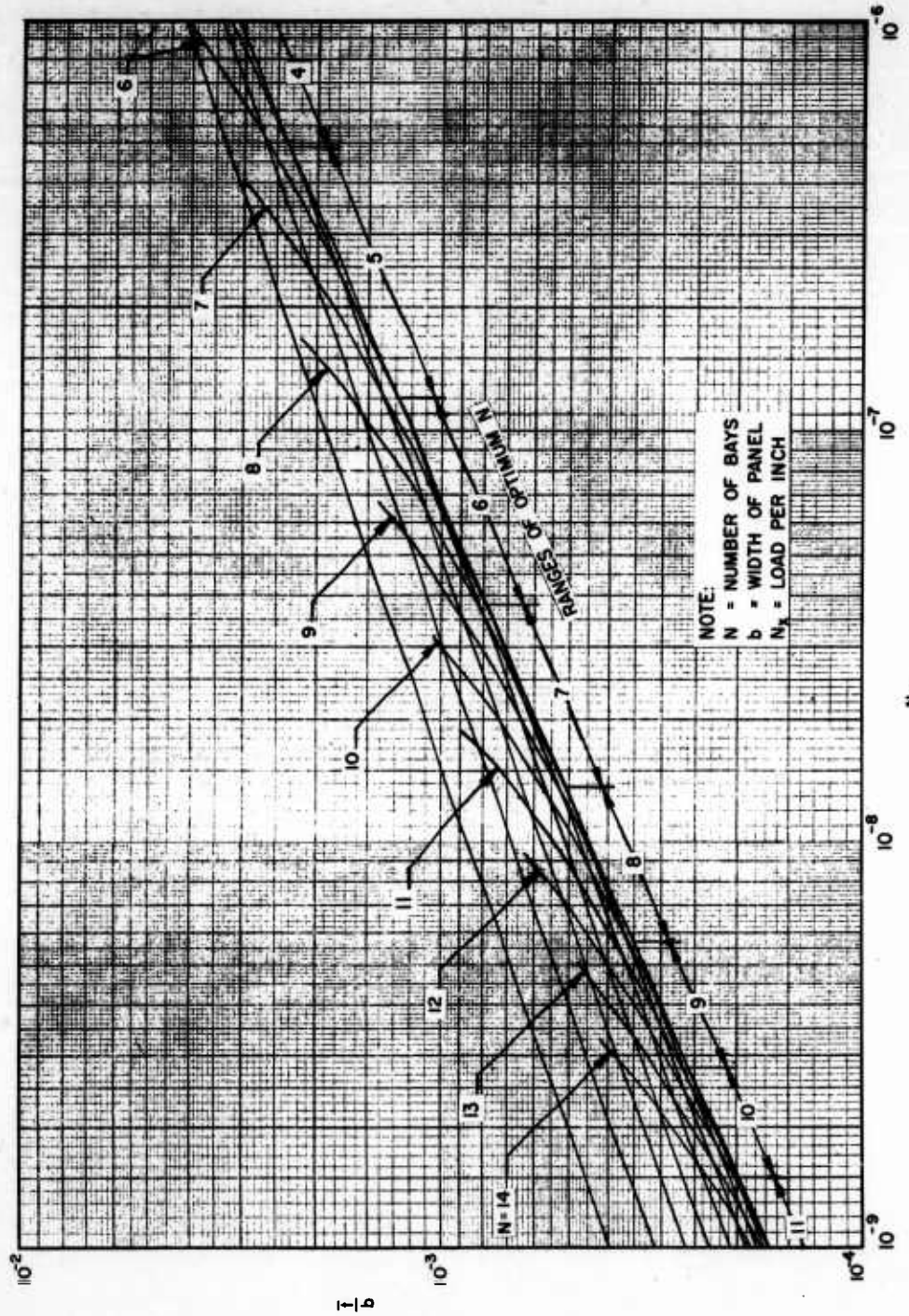

Fig. 2-6a Efficiency Chart for Unflanged, Integrally-Stiffened Flat Panels in Compression (Stiffeners Parallel to Load)

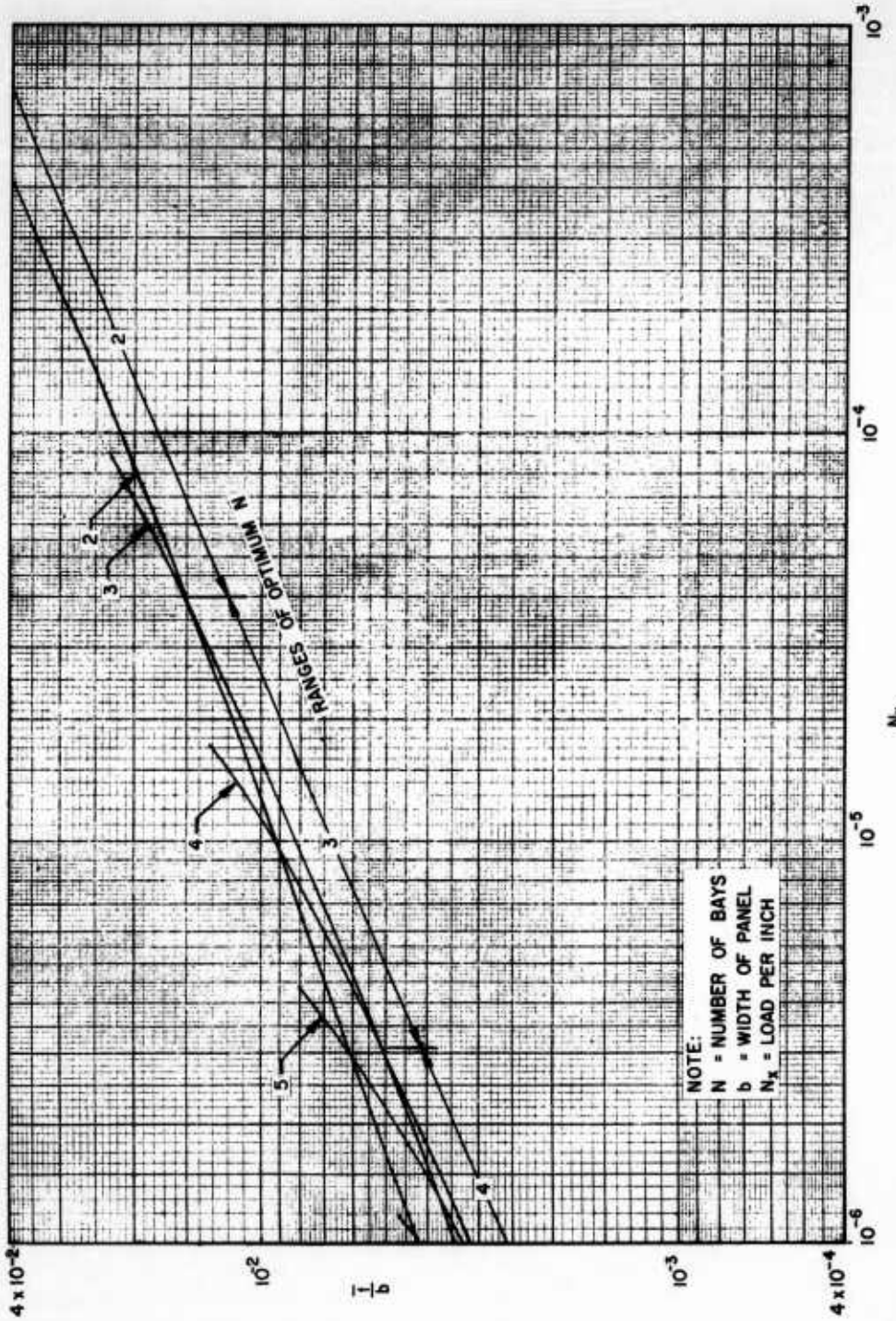

Fig. 2-6b Efficiency Chart for Unflanged, Integrally-Stiffened Flat Panels in Compression (Stiffeners Parallel to Load) (Continuation of Fig. 2.6a)

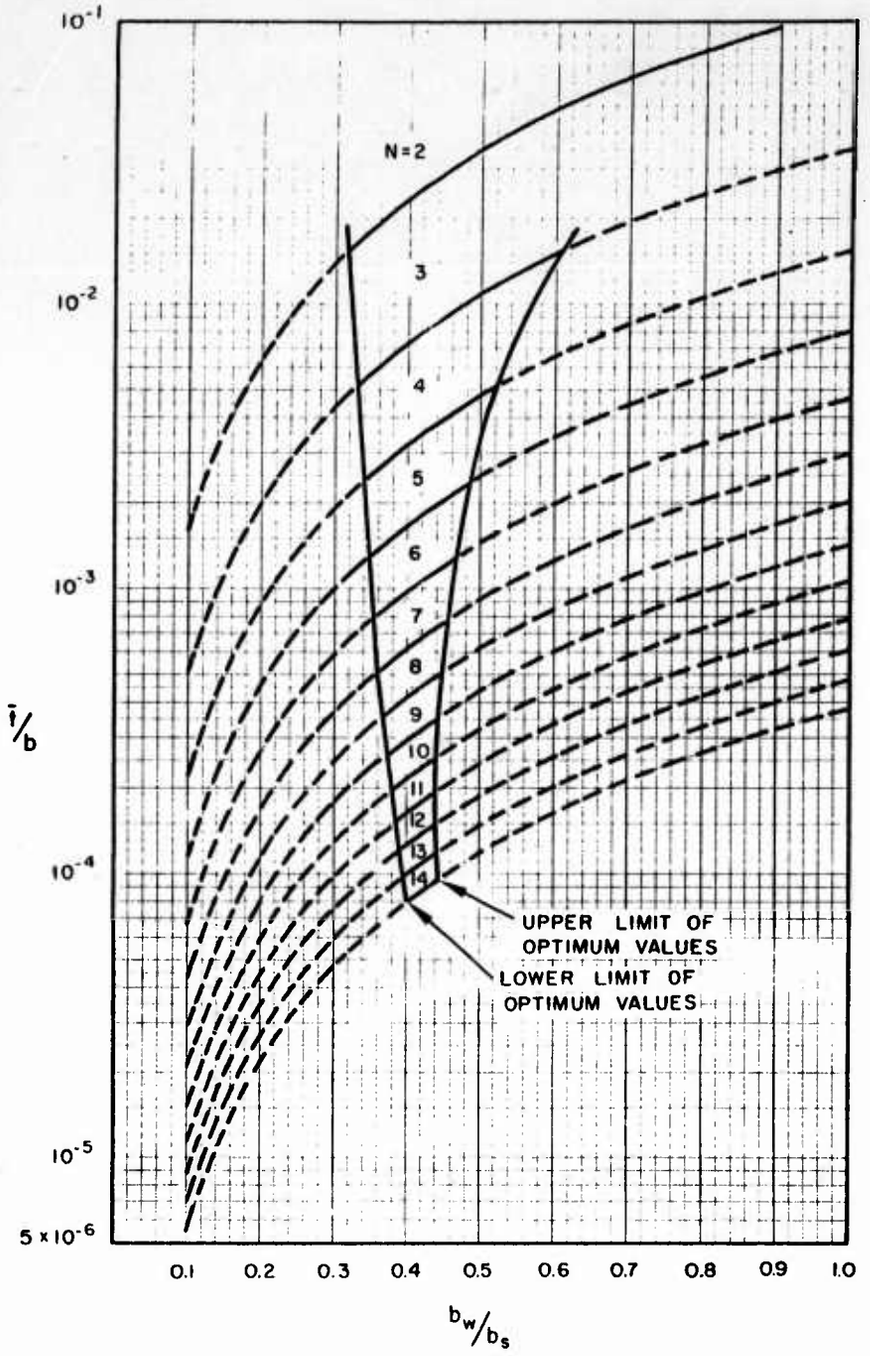

Fig. 2-7 Auxiliary Design Chart for Unflanged, Integrally-Stiffened Flat Panels in Compression

2.3 ANALYSIS OF TRUSS-CORE SEMI-SANDWICH FLAT PANELS

The minimum weight analysis for this type of panel is based on assumptions as follows:

(1) All sides of the panel are simply supported.

(2) The core consists of enough corrugations to allow the use of orthotropic plate theory in analyzing the general mode of instability.

(3) The core of the panel is composed of straight line elements.

(4) Buckling in the local mode occurs with rotation of the joints but with no deflection of the joints.

(5) $\mu = 0.3$

Values of the buckling coefficient, K_X, for the local mode of instability are presented in Ref. 9 as a function of θ and t_c/t_f for the full sandwich case and are assumed to give a close approximation for the semi-sandwich case. The cross-section of the construction is illustrated in Fig. 2-8.

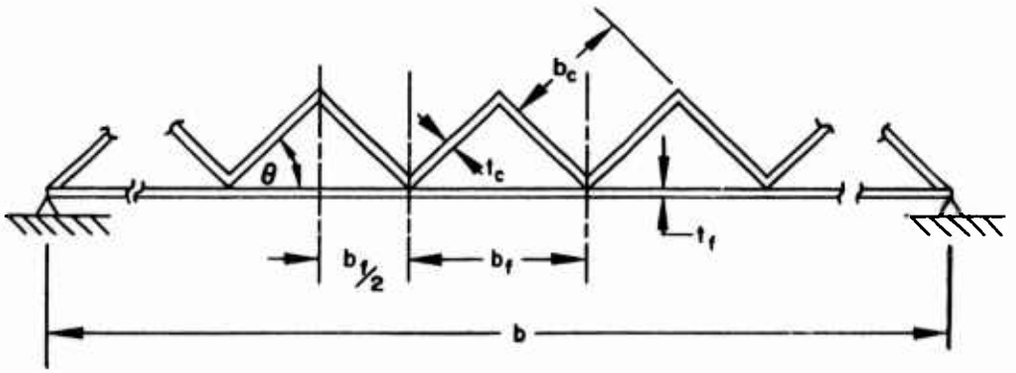

Fig. 2-8 Cross-Sectional Geometry of a Truss-Core Semi-Sandwich Panel

A derivation based on the above geometry and assumptions yields:

$$\frac{t}{b} = \frac{\sqrt{0.542\,\frac{\sigma}{\eta_G E}}\left[1 + \frac{t_c}{t_f}\,\frac{1}{\cos\theta}\right]^{3/2}}{\left\{\sqrt{1 + \frac{0.206\,K_X}{\frac{\sigma}{\eta_L E}}\left(\frac{t_c}{t_f}\right)\frac{\tan^2\theta}{\cos\theta}\left[1 + \frac{3}{1 + \frac{t_c}{t_f}\,\frac{1}{\cos\theta}}\right]\left[1 + \left(\frac{t_c}{t_f}\right)^3\cos\theta\right]} + \frac{1}{3}\left[1 + \left(\frac{t_c}{t_f}\right)^3\cos\theta\right] + \frac{0.462\,K_X\tan^2\theta}{\frac{\sigma}{\eta_L E}\left[1 + \frac{t_c}{t_f}\cos\theta\right]}\right\}^{1/2}} \qquad (2.39)$$

It is desirable to collect the various plasticity reduction factors and replace them with an effective plasticity reduction factor $\bar{\eta}$, where $\bar{\eta} = \sqrt{\eta_L \eta_G}$. Thus, the following form of Eq. (2.39) may be written:

$$\frac{t}{b} = \frac{\sqrt{0.542\,\frac{\sigma}{\bar{\eta} E}}\left[1 + \frac{t_c}{t_f}\,\frac{1}{\cos\theta}\right]^{3/2}}{\left\{\frac{\eta_G}{\bar{\eta}}\sqrt{1 + \frac{0.206\,K_X}{\frac{\sigma}{\eta_L E}}\left(\frac{t_c}{t_f}\right)\frac{\tan^2\theta}{\cos\theta}\left[1 + \frac{3}{1 + \frac{t_c}{t_f}\,\frac{1}{\cos\theta}}\right]\left[1 + \left(\frac{t_c}{t_f}\right)^3\cos\theta\right]} + \frac{\eta_G}{3\bar{\eta}}\left[1 + \left(\frac{t_c}{t_f}\right)^3\cos\theta\right] + \frac{0.462\,K_X\tan^2\theta}{\frac{\sigma}{\bar{\eta} E}\left[1 + \frac{t_c}{t_f}\,\frac{1}{\cos\theta}\right]}\right\}^{1/2}} \qquad (2.40)$$

The value of $\bar{\eta}$ to be used in this analysis is taken from Ref. 3 pertaining to truss-core sandwich panels and is assumed to apply to truss-core semi-sandwich panels as well:

$$\bar{\eta} = \left[\frac{2\eta_T^2}{1 + \eta_T}\right]^{1/4} \qquad (2.41)$$

Equation (2.41) is based on the following relationships for η_G and η_L:

$$\eta_G = \sqrt{\frac{2\eta_T}{1 + \eta_T}} \tag{2.42}$$

$$\eta_L = \sqrt{\eta_T} \tag{2.43}$$

Substituting Eqs. (2.41) through (2.43) into the denominator of Eq. (2.40), the resulting equation is:

$$\frac{\bar{t}}{b} = \frac{\sqrt{0.542\,\frac{\sigma'}{\eta E}}\left[1 + \frac{t_c}{t_f}\,\frac{1}{\cos\theta}\right]^{3/2}}{\left\{\left[\frac{2}{1+\eta_T}\right]^{1/4}\sqrt{1 + \frac{0.206\,K_X}{\left[\frac{2}{1+\eta_T}\right]^{1/4}\frac{\sigma'}{\eta E}}\left(\frac{t_c}{t_f}\right)\frac{\tan^2\theta}{\cos\theta}\left[\frac{3}{1 + \frac{t_c}{t_f}\,\frac{1}{\cos\theta}}\right]\left[1 + \left(\frac{t_c}{t_f}\right)^3\cos\theta\right]} + \frac{1}{3}\left[\frac{2}{1+\eta_T}\right]^{1/4}\left[1 + \left(\frac{t_c}{t_f}\right)^3\cos\theta\right] + \frac{0.462\,K_X\tan^2\theta}{\frac{\sigma'}{\eta E}\left[1 + \frac{t_c}{t_f}\,\frac{1}{\cos\theta}\right]}\right\}^{1/2}} \tag{2.44}$$

It is evident that is is mathematically impossible to transform all the plasticity reduction factors into effective plasticity reduction factors, $\overline{\eta}$. However, it may be shown that the quantity

$$\left[\frac{2}{1 + \eta_T}\right]^{1/4}$$

is sufficiently close to unity for practical values of η_T that it may be considered unity. It is noted that without the above simplification, the optimum geometric proportions would not be independent of material properties in the plastic stress range.

On this basis, then, the equation from which optimum geometric proportions are determined is:

$$\frac{\bar{t}}{b} = \frac{\sqrt{0.342\,\frac{\sigma}{\bar{\eta}E}}\left[1 - \frac{t_c}{t_f}\frac{1}{\cos\theta}\right]^{3/2}}{\left\{\sqrt{1 - \frac{0.206\,K_x\left(\frac{t_c}{t_f}\right)\tan^2\theta}{\frac{\sigma}{\bar{\eta}E}\cos\theta}\left[1 + \frac{3}{1 - \frac{t_c}{t_f}\frac{1}{\cos\theta}}\right]\left[1 - \left(\frac{t_c}{t_f}\right)^3\cos\theta\right]} - \frac{1}{3}\left[1 - \left(\frac{t_c}{t_f}\right)^3\cos\theta\right] - \frac{0.462\,K_x\tan^2\theta}{\frac{\sigma}{\bar{\eta}E}\left[1 - \frac{t_c}{t_f}\frac{1}{\cos\theta}\right]}\right\}^{1/2}} \tag{2.45}$$

Equation (2.45) may be used in conjunction with Eq. (2.9) to determine $N_x/b\bar{\eta}E$.

It is demonstrated later that the order of magnitude of the first and second terms in the denominator of Eq. (2.45) is negligible over the practical range of $N_x/b\bar{\eta}E$. Consequently, Eq. (2.45) may be approximated in such a manner that the ideal form of Eq. (2.1) results:

$$\frac{N_x}{b\bar{\eta}E} = \left[\frac{0.924\sqrt{K_x}\tan\theta}{\left(1 + \frac{t_c}{t_f}\frac{1}{\cos\theta}\right)^2}\right]\left(\frac{\bar{t}}{b}\right)^2 \tag{2.46}$$

In view of the form of Eq. (2.46), the minimum weight proportions may be found by maximizing $\mathcal{E}$, where:

$$\mathcal{E} = \frac{0.924\sqrt{K_x}\tan\theta}{\left(1 + \frac{t_c}{t_f}\frac{1}{\cos\theta}\right)^2} \tag{2.47}$$

Figure 2-9 shows that the maximum value of $\mathcal{E}$ occurs when θ is approximately 47.5°, and t_c/t_f is approximately 0.49. These values of θ and t_c/t_f produce minimum weight regardless of the magnitude of the load. Note, however, that some

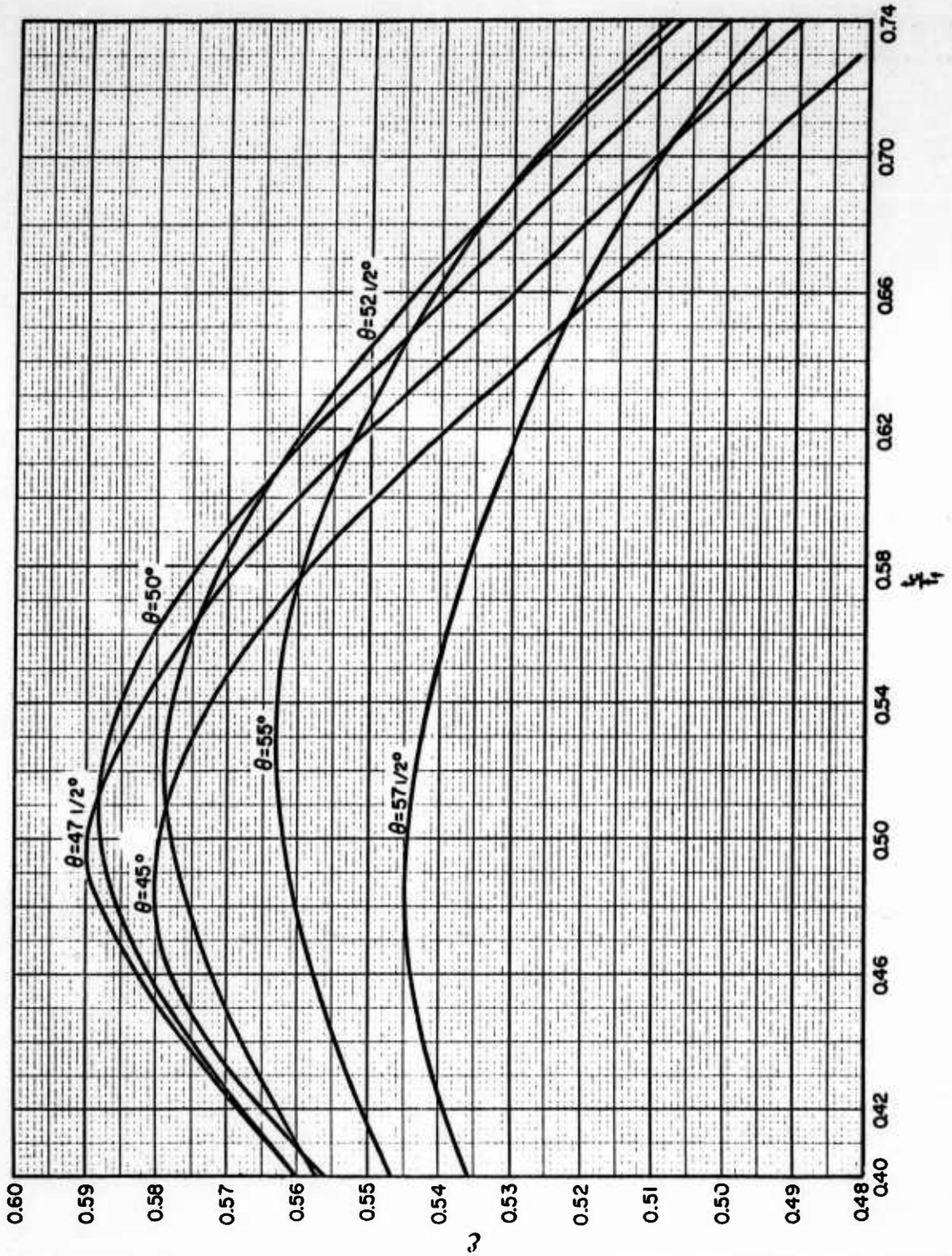

Fig. 2-9 Efficiency Chart for Truss-Core Semi-Sandwich Panels (Corrugations Parallel to Load)

less efficient geometries produce values of $\mathcal{E}$ which nearly equal the maximum value. Equations necessary for general design are:

$$\frac{N_x}{b\bar{\eta}E} = \mathcal{E}\left(\frac{\bar{t}}{b}\right)^2 \tag{2.48}$$

$$t_f = \frac{\bar{t}}{\left(1 + \frac{t_c}{t_f}\frac{1}{\cos\theta}\right)} \tag{2.49}$$

$$b_f = 0.95\, t_f \sqrt{\frac{K_x\left(\frac{\bar{t}}{b}\right)}{\frac{N_x}{b\eta_L E}}}\,, \quad \text{where} \quad \eta_L = \sqrt{\eta_T} \tag{2.50}$$

$$b_c = \frac{b_f}{2\cos\theta} \tag{2.51}$$

For minimum weight design, these equations reduce to:

$$\frac{N_x}{b\bar{\eta}E} = 0.59\left(\frac{\bar{t}}{b}\right)^2 \tag{2.52}$$

$$t_f = 0.58\,\bar{t} \tag{2.53}$$

$$b_f = 0.95\, t_f \sqrt{\frac{3.03\left(\frac{\bar{t}}{b}\right)}{\frac{N_x}{b\eta_L E}}}\,, \quad \text{where} \quad \eta_L = \sqrt{\eta_T} \tag{2.54}$$

$$b_c = 0.74\, b_f \tag{2.55}$$

Note that Eqs. (2.50) and (2.54) are a function of η_L rather than $\bar{\eta}$. Values of η_L may be derived from material tangent modulus charts presented in the literature or from the Ramberg-Osgood formulation for tangent modulus (Ref. 6).

In those designs where $N_x/b\bar{\eta}E$ exceeds 10^{-4}, it is desirable to assess the effect of the approximation which allowed Eq. (2.46) to be written. Figure 2-10 shows that the approximation is always conservative, and that the degree of conservatism can be significant. It is recommended that Fig. 2-10 be used in place of Eq. (2.52) when $N_x/b\bar{\eta}E > 10^{-4}$. While $\bar{t}/b$ in Fig. 2-10 applies only to the minimum weight panel proportions, the percent error may be assumed to apply to all non-optimum panel proportions. Thus, when $N_x/b\bar{\eta}E > 10^{-4}$, Eq. (2.48) becomes:

$$\frac{N_x}{b\bar{\eta}E} = \mathcal{E}\left[\frac{\bar{t}/b}{\frac{\%\ \text{Error}}{100} + 1}\right]^2 \qquad (2.56)$$

2.4 ANALYSIS OF TRUSS-CORE SANDWICH FLAT PANELS

The truss-core sandwich panel construction treated in this subsection has the same geometry as illustrated in Fig. 2-8, with the addition of a second face plate on the open side of the core which is identical to the existing face plate. This construction has been the subject of a comprehensive minimum weight analysis, reported in Ref. 3. The equations and charts presented here are taken from that reference. All assumptions set forth in subsection 2.3 apply to this construction also.

As seen in Eq. (2.57), minimum weight results when the combinations of θ and t_c/t_f are determined which yield the maximum value of $N_x/b\bar{\eta}E$ for a given value of $\bar{t}/b$. It is noted that K_X, the local buckling coefficient, is presented in Ref. 9 as a function of θ and t_c/t_f.

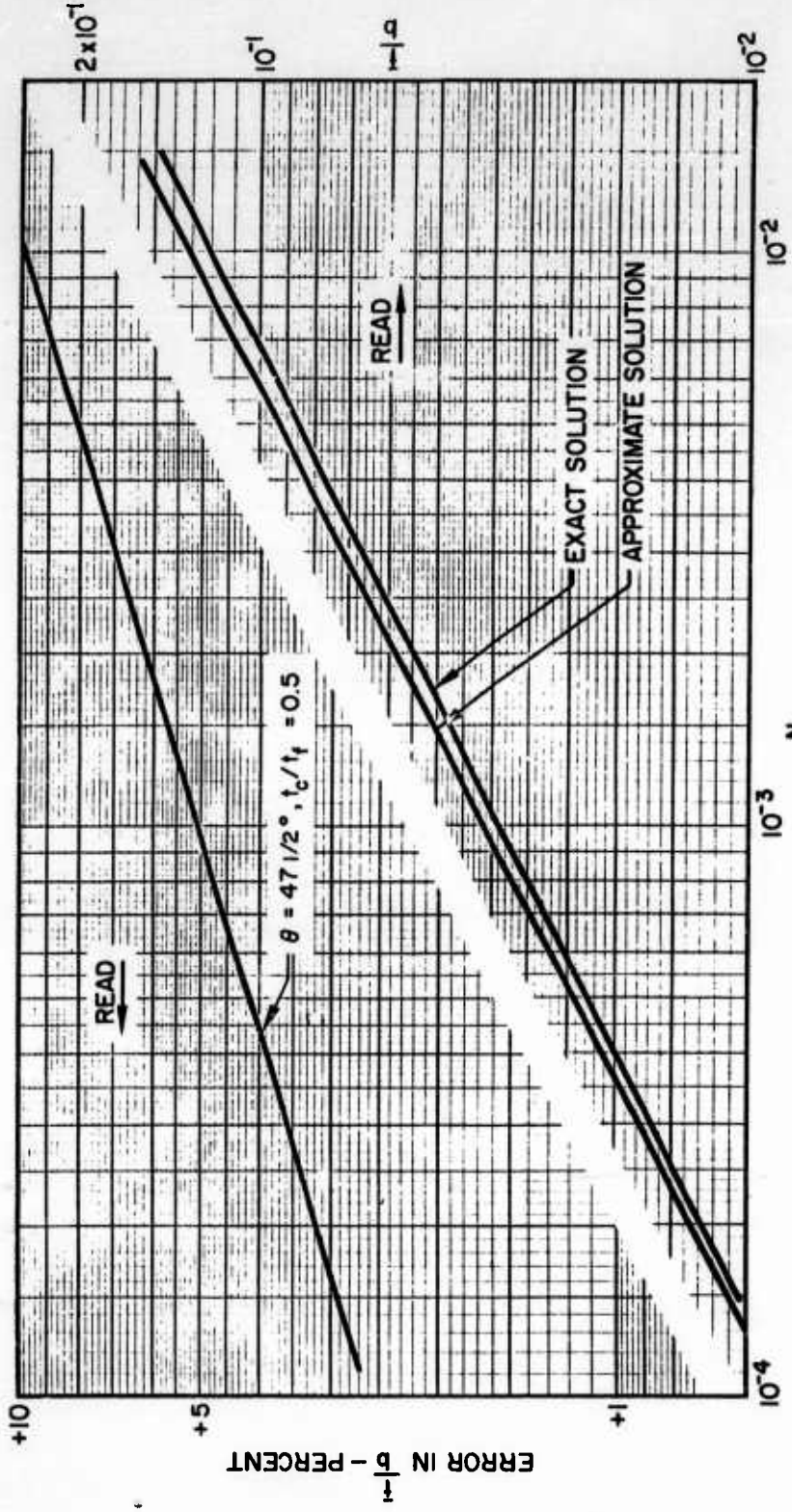

Fig. 2-10 Comparison Between Exact and Approximate Truss-Core Semi-Sandwich Panel Solutions at High Loading-Material Indexes (Corrugations Parallel to Load)

$$\frac{N_x}{b\bar{\eta}E} = \frac{1.565\sqrt{K_x}\tan\theta\left[1+\sqrt{1+0.152\,\frac{t_c}{t_f}\,\frac{1}{\cos\theta}}\right]^{1/2}\left(\frac{\bar{t}}{b}\right)^2}{\left[2+\frac{t_c}{t_f}\,\frac{1}{\cos\theta}\right]^{3/2}} - \frac{2.910\,K_x\left[1+0.152\,\frac{t_c}{t_f}\,\frac{1}{\cos\theta}\right]\left(\frac{\bar{t}}{b}\right)^3}{\frac{t_c}{t_f}\cos\theta\left[2+\frac{t_c}{t_f}\,\frac{1}{\cos\theta}\right]^2} \tag{2.57}$$

The effective plasticity factor $\bar{\eta}$ is given by Eq. (2.41).

It is demonstrated in Ref. 3 that Eq. (2.57) may be simplified, when $N_x/b\bar{\eta}E < 10^{-4}$, to the form shown in Eq. (2.58):

$$\frac{N_x}{b\bar{\eta}E} = \left[\frac{1.565\sqrt{K_x}\tan\theta\left[1+\sqrt{1+0.152\,\frac{t_c}{t_f}\,\frac{1}{\cos\theta}}\right]^{1/2}}{\left[2+\frac{t_c}{t_f}\,\frac{1}{\cos\theta}\right]^{3/2}}\right]\left(\frac{\bar{t}}{b}\right)^2 \tag{2.58}$$

Equation (2.58) is of the form of Eq. (1). Therefore:

$$\mathcal{E} = \frac{1.565\sqrt{K_x}\tan\theta\left[1+\sqrt{1+0.152\,\frac{t_c}{t_f}\,\frac{1}{\cos\theta}}\right]^{1/2}}{\left[2+\frac{t_c}{t_f}\,\frac{1}{\cos\theta}\right]^{3/2}} \tag{2.59}$$

The maximization of $\mathcal{E}$ in Eq. (2.59) produces minimum weight proportions. Figure 2-11 shows that the maximum value of $\mathcal{E}$ is 1.108 and that it occurs when θ is approximately 60° and t_c/t_f approximately 0.83. Note that several other combinations of θ and t_c/t_f produce values of $\mathcal{E}$ which are very close to the maximum.

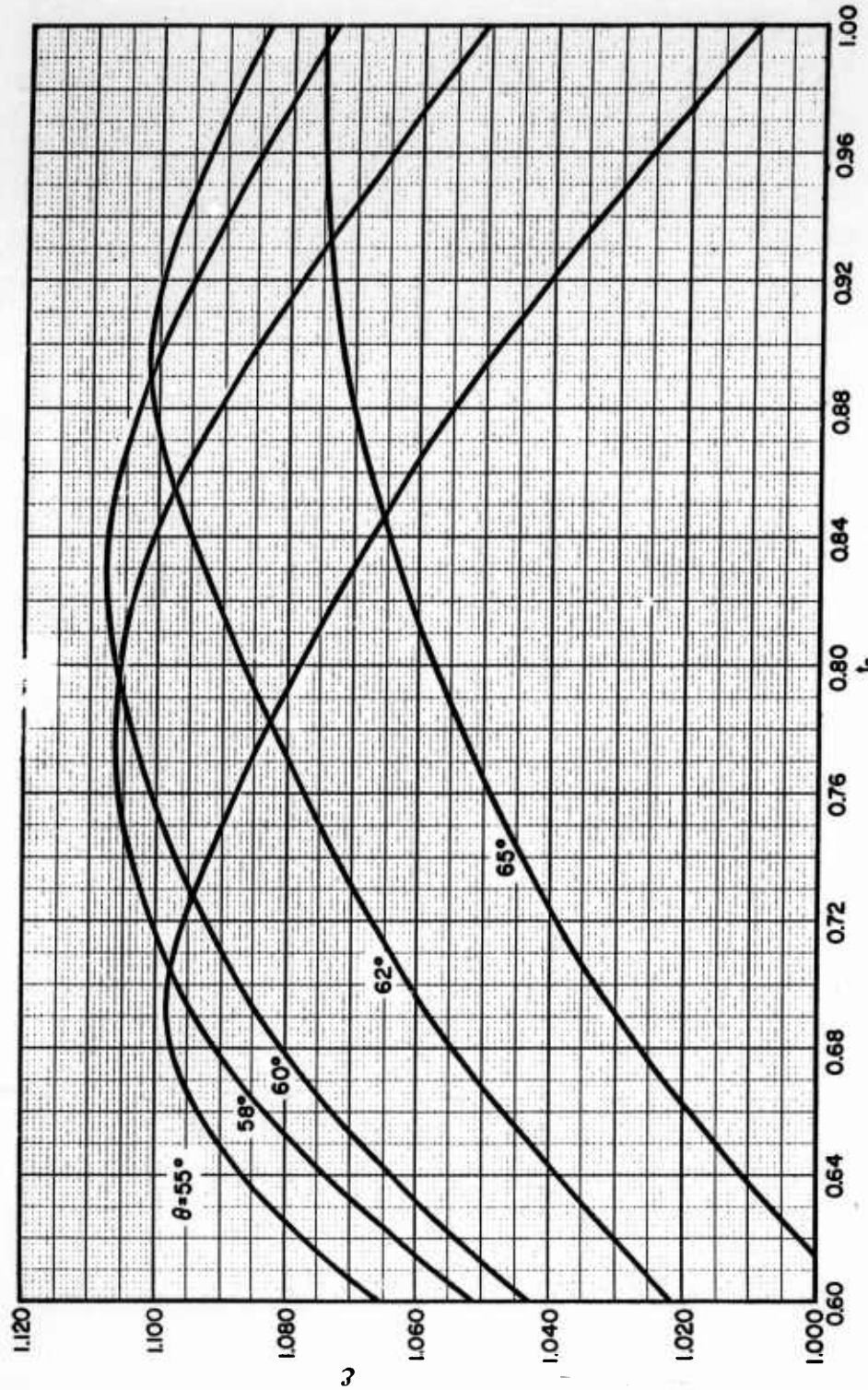

Fig. 2-11 Efficiency Chart for Truss-Core Sandwich Panels (Corrugations Parallel to Load)

Equations necessary for general design purposes for this construction are identical to Eqs. (2.48), (2.50) and (2.51), presented in the previous section, together with Eq. (2.60):

$$t_f = \frac{\bar{t}}{2 + \frac{t_c}{t_f}\frac{1}{\cos\theta}} \tag{2.60}$$

These equations reduce to the following forms for minimum weight design:

$$\frac{N_x}{b\bar{\eta}E} = 1.108\left(\frac{\bar{t}}{b}\right)^2 \tag{2.61}$$

$$t_f = 0.273\,\bar{t} \tag{2.62}$$

$$b_f = 0.95\,t_f\sqrt{\frac{3.40\,(\bar{t}/b)}{\left(\frac{N_x}{b\eta_L E}\right)}} \tag{2.63}$$

where

$$\eta_L = \sqrt{\eta_T}$$

$$b_c = b_f \tag{2.64}$$

It is shown in Ref. 3 that the practical range of application of sandwich construction is for low loadings, or, when $N_x/b\bar{\eta}E < 10^{-4}$. Consequently, information for those cases where $N_x/b\bar{\eta}E > 10^{-4}$ is not presented.

Section 3

RELATIVE EFFICIENCIES OF THE SEVERAL TYPES OF PANEL CONSTRUCTION

A comparison of the maximum efficiencies of the four panel constructions of the preceding section is presented in Fig. 3-1, based on Figs. 2-2a, 2-2b, and 2-6a, 2-6b and Eqs. (2.52) and (2.61). A flat,unstiffened plate is also presented [Eq. (A.2)]. It is apparent that the truss-core sandwich panel construction is superior to the other constructions for the range of loading-material index considered. This is particularly true for low loads; for example, when $N_x/b\bar{\eta}E = 2 \times 10^{-8}$, truss core sandwich is more than ten times lighter than an unstiffened plate, and approximately four times lighter than a zee-stiffened panel. The truss-core semi-sandwich panel construction, while offering the most competition to the truss-core sandwich of the other constructions considered, is still heavier by 30 percent at this same loading-material index. At high loading-material indexes, the superiority of the truss-core sandwich diminishes, and careful attention should be given to the cost per pound of weight saved when using sandwich, as well as to plasticity effects. The effects of plasticity are best illustrated by removing the material parameter $\bar{\eta}E$ from the loading-material index and incorporating it into the envelopes. This has been done in Fig. 3-2 for 17-7PH (Cond. TH-1050) steel. It is apparent from this chart that all constructions move rapidly toward a common efficiency when each reaches the maximum stress level, taken here to be the compressive yield stress. Thus, referring to Fig. 3-2, truss-core sandwich and truss-core semi-sandwich are seen to have equal efficiency above some value of N_x/b, the exact value being a function of material and thermal environment.

Figure 3-1 shows that, at extremely high loadings, all envelopes converge towards the flat,unstiffened plate. This convergence is clearly demonstrated when plasticity

effects are included, as in Fig. 3-2. As before, the exact value of N_x/b, above which the flat, unstiffened plate is as efficient as the stiffened panels, is a function of material and thermal environment.

Generally speaking, few designs require $\bar{t}/b \geq 10^{-1}$, since such a value calls for extremely high design stresses, quite unrealistic in missile and spacecraft structures. Therefore, a flat, unstiffened plate is seldom the best choice. It should be noted that the minimum weight envelopes for the zee-stiffened panel and the unflanged integrally-stiffened panel are approximately equivalent. It is surmised that other conventional stiffener shapes will produce minimum weight envelopes which are closely related to those shown; i.e., while efficiency may improve slightly with other non-sandwich stiffener shapes, it will not compete with sandwich construction efficiency over the range of the $N_x/b\bar{\eta}E$ considered.

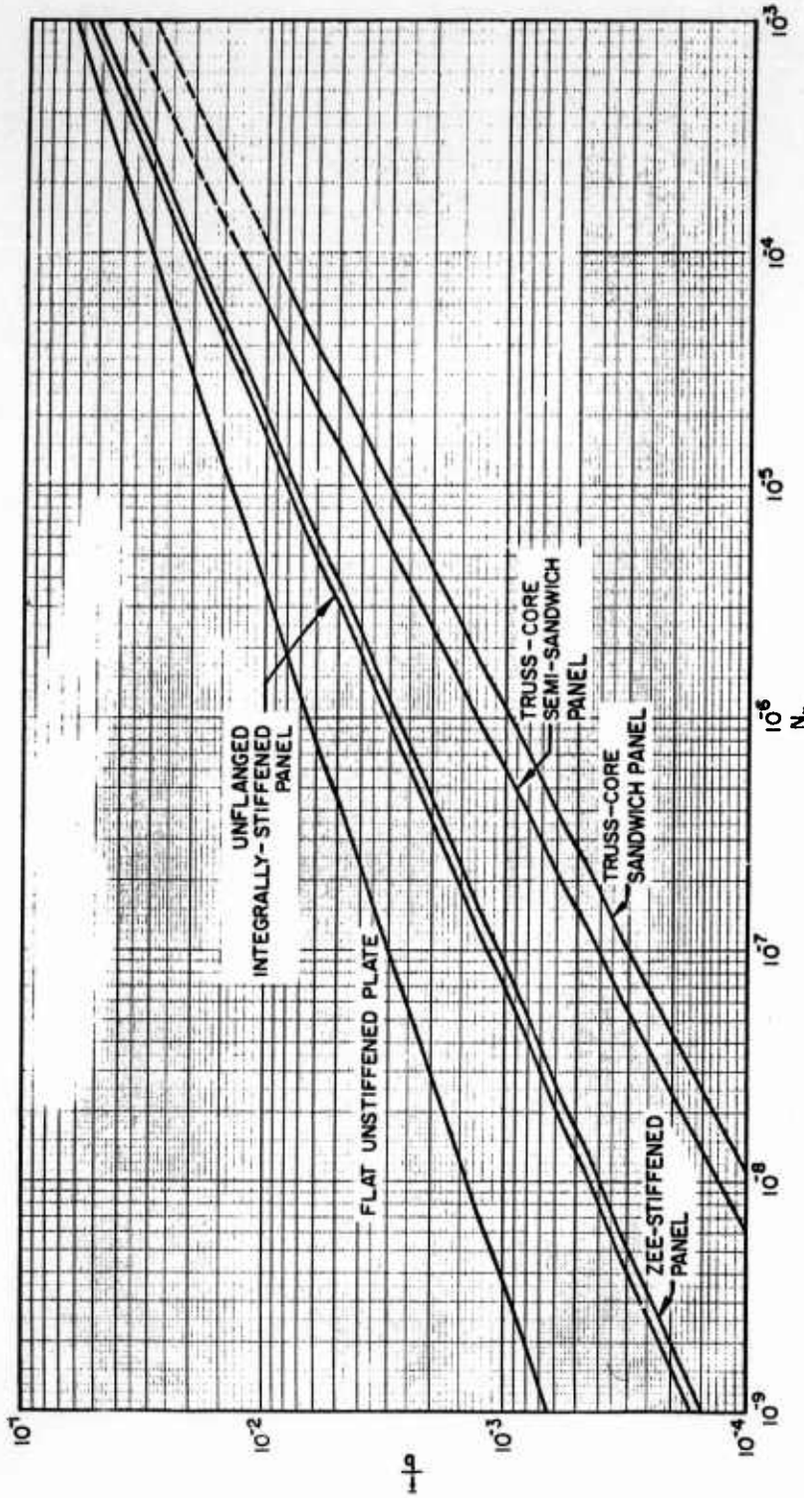

Fig. 3-1 Comparison of the Minimum Weight Envelopes of the Several Types of Stiffened Panel Construction when Subjected to a Compression Load in the Direction of the Stiffening Elements

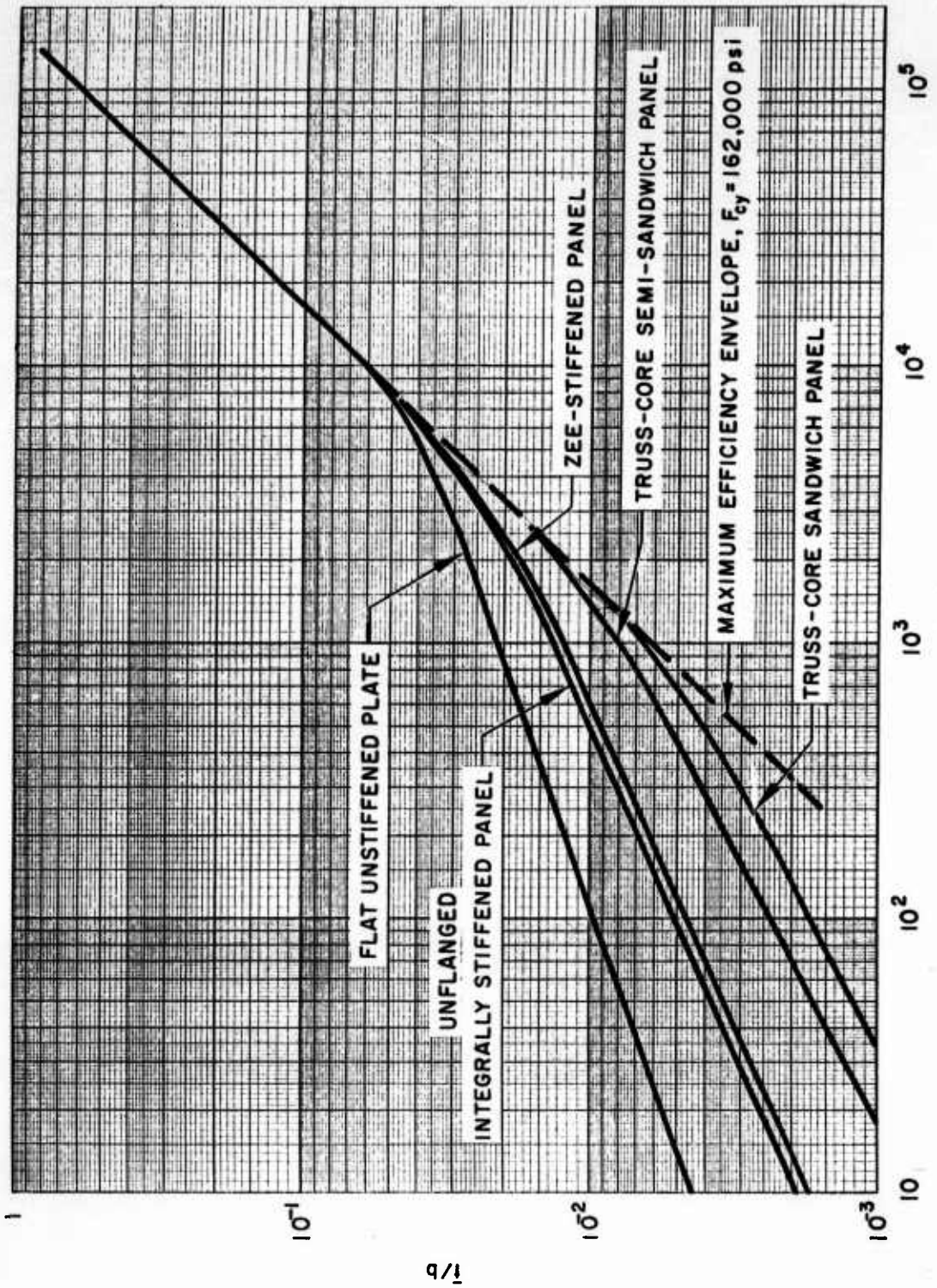

Fig. 3-2 Design Chart for Minimum Weight 17-7PH (Cond. TH-1050) Steel Panels in Compression (Room Temperature)

Section 4
CONCLUSIONS

Conclusions from the analyses are presented, together with matters of recommendation, as follows:

1. The mathematically determined minimum-weight geometries developed are based on idealizations which may not be duplicated in practical applications because of the likely presence of additional loads, criteria, and peculiar edge conditions, or the impracticability of the indicated minimum weight gages and proportions. However, the design charts presented do establish the trends for efficient design and these are useful in establishing the quality of a practical design from the weight point of view.
2. Of the four stiffened-panel constructions investigated, the truss-core sandwich panel construction produces minimum weight over the practical range of the loading-material index. However, based on a comparison of these constructions wherein plasticity effects have been incorporated, it is concluded that truss-core sandwich should be used primarily in elastic stress applications.
3. The truss-core, semi-sandwich construction is competitive with truss-core sandwich construction, being only approximately 30 percent heavier for all practical loadings yet more economical to produce. It should receive serious attention only when uniaxial loads are to be carried.
4. The conventionally stiffened panels treated in this report produce minimum weight envelopes which are closely related to each other and which are not competitive with the sandwich constructions presented, for all practical design applications.
5. To accurately evaluate minimum-weight, stiffened, compression panels for a given material, charts of $\bar{t}/b$ versus N_x/b are recommended. This type of chart clearly shows the loading index range where, because of

plasticity effects, all constructions yield similar efficiencies, and therefore, the flat unstiffened plate is the best choice. It is noted, however, that this loading index range is generally above the usual loading index range for missile and spacecraft structures.

6. The efficiency charts presented in this report may be used for stress analysis, as well as for structural design, owing to the presentation of non-optimum data.
7. Testing of minimum-weight geometries for the four types of stiffened compression panels discussed in this report is recommended to substantiate the theoretical results. Test data now available are sufficient to substantiate only the theoretical minimum weight analysis of zee-stiffened wide-columns. Experimental verification of orthotropic plate theory as applied to the constructions considered in this report also is recommended.

Section 5

REFERENCES

1. Journal of the Aeronautical Sciences, Effects of Material Distribution on Strength of Panels, by Adam Zahorski, Vol. 11, No. 3, pp. 247-253, Jul 1944
2. Weight-Strength Analysis of Aircraft Structures, by F. R. Shanley, McGraw-Hill Book Co., Inc., New York, N Y., 1952
3. Lockheed Missiles and Space Division, Minimum Weight Analyses and Design Procedures for Flat, Truss-Core Sandwich Panels, by R. F. Crawford, A. B. Burns, and L. K. Tilcens, LMSD-704009, Sunnyvale, Calif., Aug 1960
4. Lockheed Missiles and Space Division, Structural Methods Handbook, LMSD-895078, Sunnyvale, Calif., Apr 1960
5. National Advisory Committee for Aeronautics, Compressive Buckling of Simply Supported Plates with Longitudinal Stiffeners, by Paul Seide and Manuel Stein, TN-1825, Washington, D. C., 1949
6. National Advisory Committee for Aeronautics, Description of Stress-Strain Curves by Three Parameters, by Walter Ramberg and William R. Osgood, TN-902, Washington, D. C., Jul 1943
7. Lockheed Missiles and Space Division, Structural Materials Handbook, LMSD-325441, Sunnyvale, Calif., Oct 1960
8. Lockheed Missiles and Space Division, The Determination of Local Crippling Allowables by IBM-7090 Machine Techniques, by A. Bruce Burns, LMSD-704012, Sunnyvale, Calif., Oct 1960
9. National Advisory Committee for Aeronautics, Local Instability of the Elements of a Truss-Core Sandwich Plate, by Melvin S. Anderson, TN 4292, Washington, D. C., Jul 1958
10. Royal Aeronautical Society, Handbook of Aeronautics, No. 1, Structural Principles and Data, by J. H. Argyris and P. C. Dunne, pp. 185-207, 4th Edition, Pitman Publishing Corporation, New York, 1952

11. Journal of the Royal Aeronautical Society, The Optimum Design of Compression Surfaces having Unflanged Integral Stiffeners, by E. J. Catchpole, Vol. 58, No. 527, pp. 765-768, London, England, Nov 1954

12. Wright Air Development Division, Design Optimization Procedures and Experimental Program for Box Beam Structures, Volume I, by Laszlo Berke and Paul L. Vergamini, WADD TR 60-149, Vol. I, Wright-Patterson Air Force Base, Ohio, Jun 1960

Appendix A
EFFICIENCY OF FLAT, UNSTIFFENED PLATES IN COMPRESSION

It is convenient, when comparing stiffened panel, minimum-weight analyses, to use a flat, unstiffened plate as a basis for comparison. In this appendix, an efficiency equation for a flat, unstiffened plate in compression is developed and shown to be a function of material selection alone. Several charts are presented which compare selected structural materials at various temperatures.

Buckling of flat unstiffened plates in compression may be determined from the familiar equation:

$$\sigma_{cr_L} = \eta_L \frac{E\pi^2}{12(1-\mu^2)} \left(\frac{t}{b}\right)^2 K_S \qquad (A.1)$$

When the edges are assumed simply supported and the plate aspect ratio is equal to or greater than unity, K_s may be set equal to 4.0. Substituting K_S into Eq. (A.1), taking $\mu = 0.3$, and rearranging results in the following form:

$$\frac{N_x}{b\bar{\eta}E} = \frac{\sigma}{\bar{\eta}E} \cdot \frac{\bar{t}}{b} = 3.62 \left(\frac{\bar{t}}{b}\right)^3 \qquad (A.2)$$

where $\bar{t} = t$, $\bar{\eta} = \eta_L$ and N_x is the load per unit width causing buckling in the plate. Equation (A.2) is the ideal nondimensionalized form, and it is shown plotted in Figs. 3-1 and 3-2. For an unstiffened plate, efficiency is a function of material selection, alone, as can be seen from Eq. (A.2) which applies for any loading-material index. In order to show the variations in efficiency, charts are developed in which the effects of material density, Young's modulus and the effective plasticity factor $\bar{\eta}$

are evaluated. This is accomplished using Eqs. (A.2) and (A.3):

$$W = \bar{t} b \rho$$

$$\frac{W}{b^2} = \frac{\bar{t}}{b} \cdot \rho \qquad \text{(A.3)}$$

and taking

$$\bar{\eta} = \sqrt{\eta_T} \qquad \text{(A.4)}$$

The resulting charts, presented in Figs. A-1 through A-5, consider the merits of several materials over a temperature range from 70° F to 1000° F, the materials exhibiting minimum values of W/b^2 being most efficient. Note that for low values of N_x/b the materials plot parallel lines as a function of E/ρ^3. A transition range follows as the buckling stresses pass the proportional limit and the materials behave according to their corresponding $\bar{\eta}$ values. The point of transition varies with each material, depending on the proportional limit stress σ_{PL}, which affects N_x/b as well as $\bar{\eta}$. It is assumed that the maximum buckling stress for all materials is the compressive yield stress. Therefore, it can be noted from Eq. (A.2) that at large values of N_x/b the quantities σ and $\bar{\eta}$ remain constant, and any increase in N_x/b must be only the result of increased weight $\bar{t}/b$. Since this represents a linear relationship, the slope of the curves changes to a 45° slope (on log-log paper) after the compressive yield stress has been reached. In this region of N_x/b, the materials plot parallel lines as a function of F_{cy}/ρ. It is seen from the charts that no single available material combines the desirable features of a high value of Young's modulus, high compressive yield stress and low density, although beryllium has a relatively high value of Young's modulus and low density which combine to make it a superior material for low and medium loading indexes. Beryllium, however, does not have a high F_{cy}/ρ, when compared to the so-called high-strength materials. As a result, it is inferior to these materials for high loading indexes. It should be noted that Figs. A-1 through A-5 are based on a mathematical analysis which assumes that the buckling

characteristics of materials are related to the compressive stress strain diagram. Also, specific mechanical and stress-strain properties have been used which are subject to variation depending upon material thickness, heat treatment, and composition. The effect of these variations may be evaluated approximately, knowing the curve section on the chart which is a function of some particular property of the material.

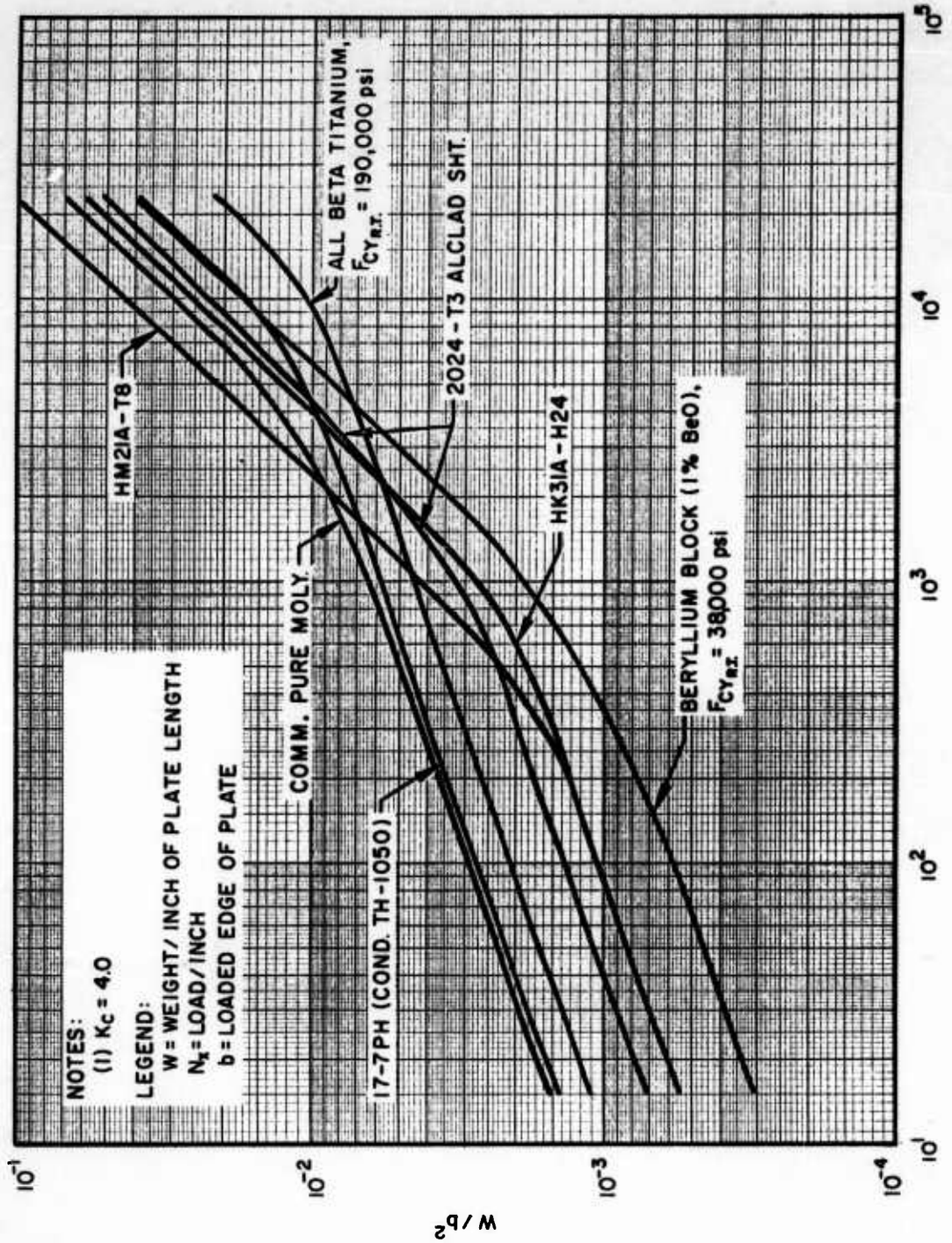

Fig. A-1 Strength-Weight Comparison of Various Sheet Alloys When Used as Flat, Unstiffened Plates in Compression at 70° F

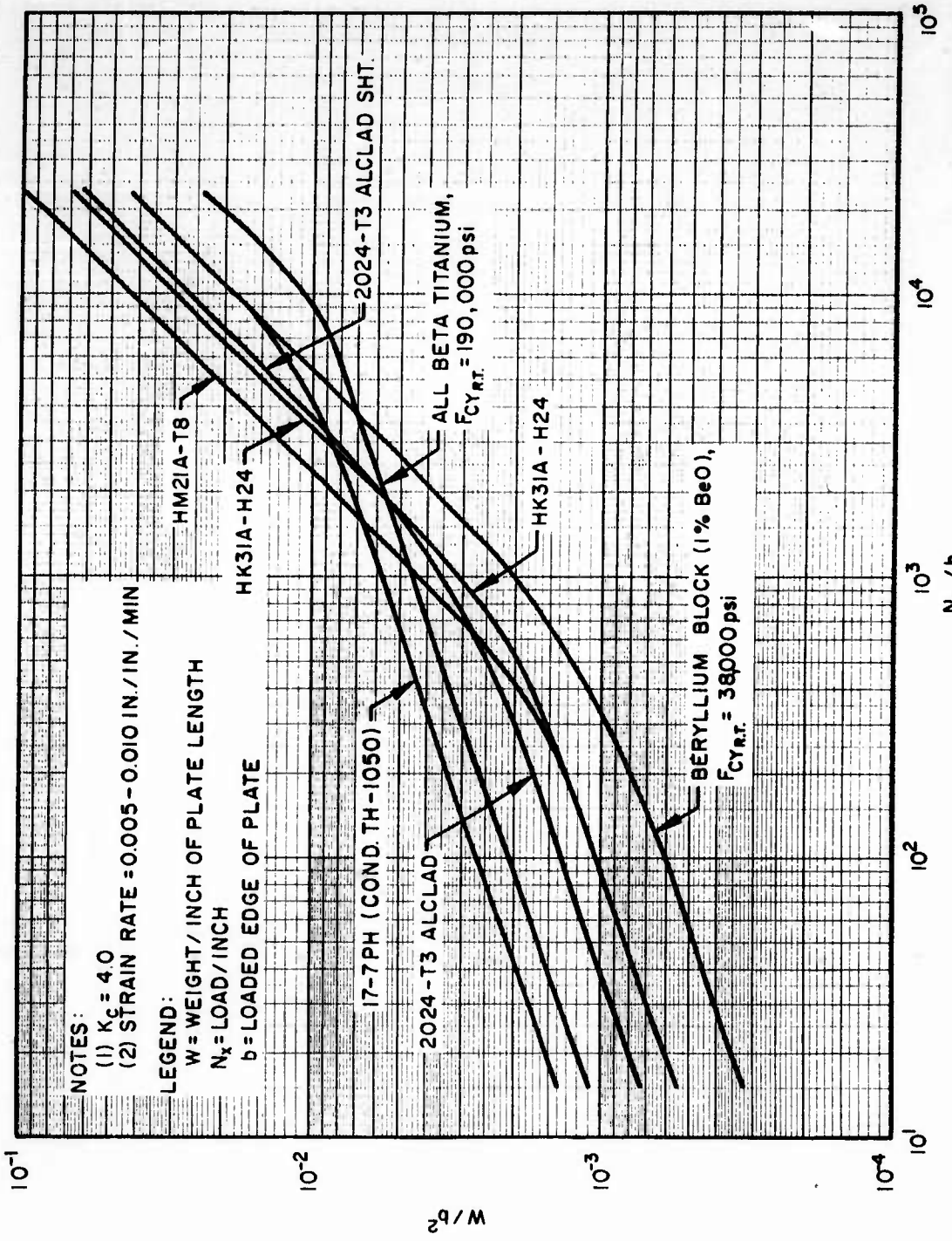

Fig. A-2 Strength-Weight Comparison of Various Sheet Alloys When Used as Flat, Unstiffened Plates in Compression at 400° F After 0.5 Hour Exposure

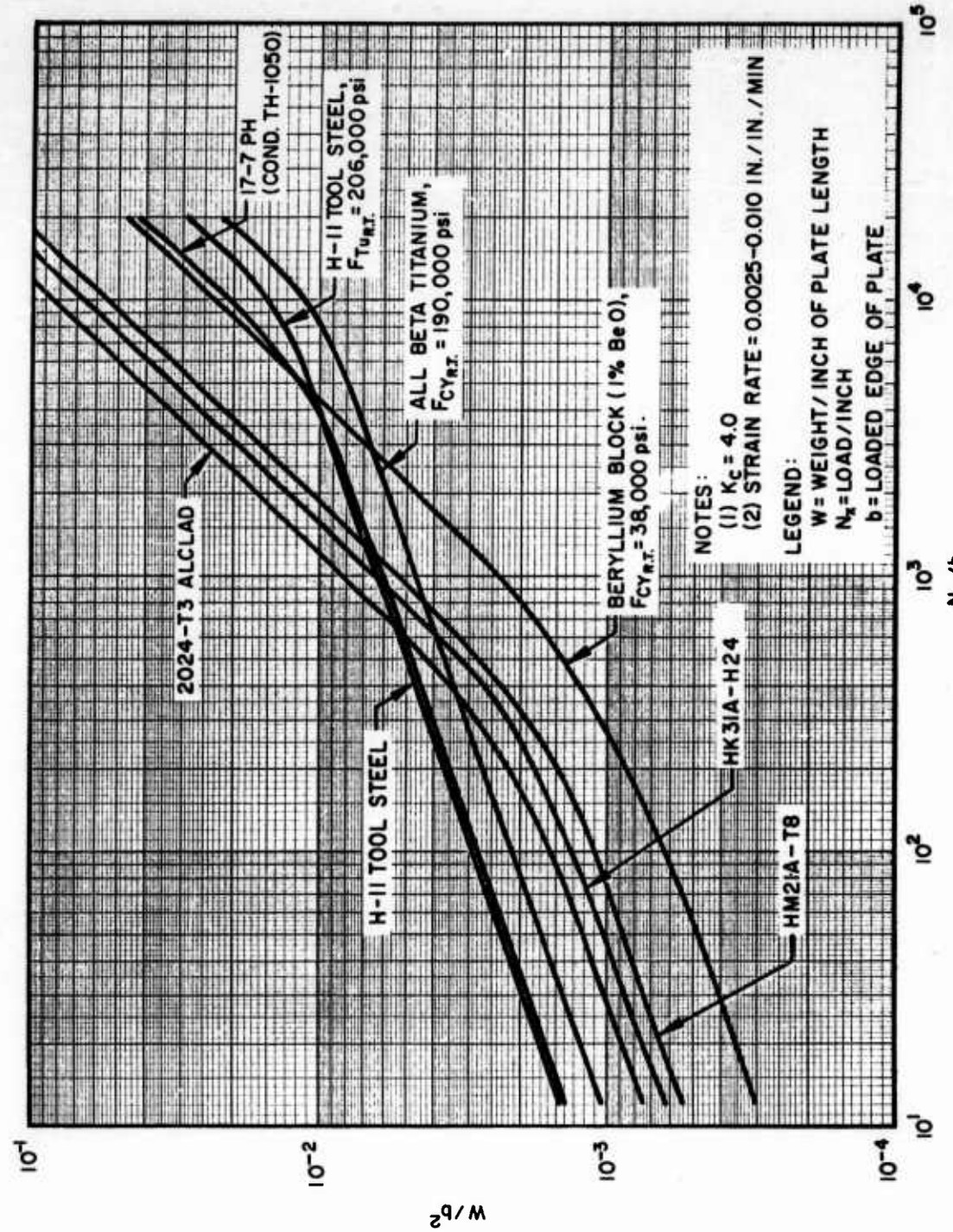

Fig. A-3 Strength-Weight Comparison of Various Sheet Alloys When Used as Flat, Unstiffened Plates in Compression at 600° F After 0.5 Hour Exposure

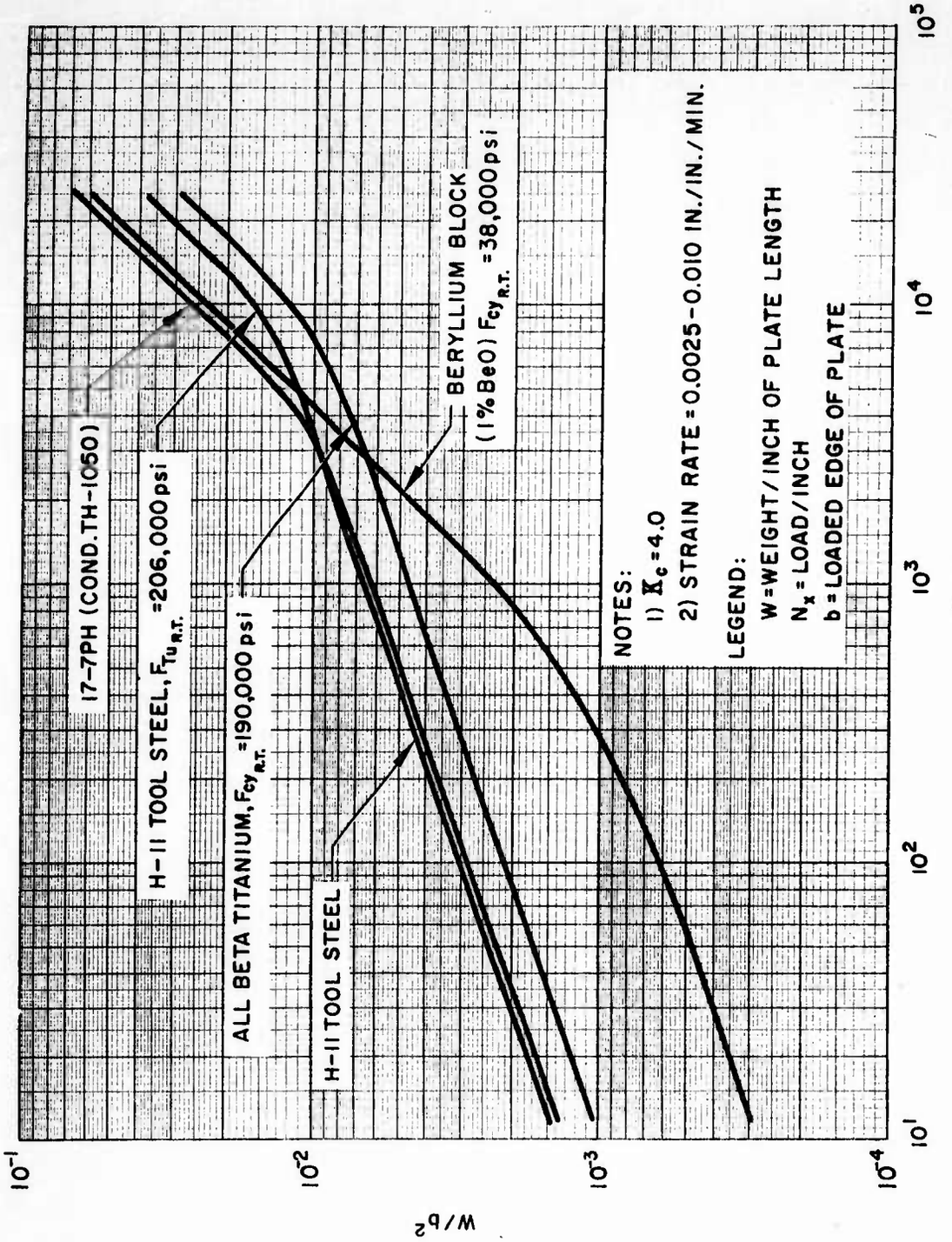

Fig. A-4 Strength-Weight Comparison of Various Sheet Alloys When Used as Flat, Unstiffened Plates in Compression at 800°F After 0.5 Hour Exposure

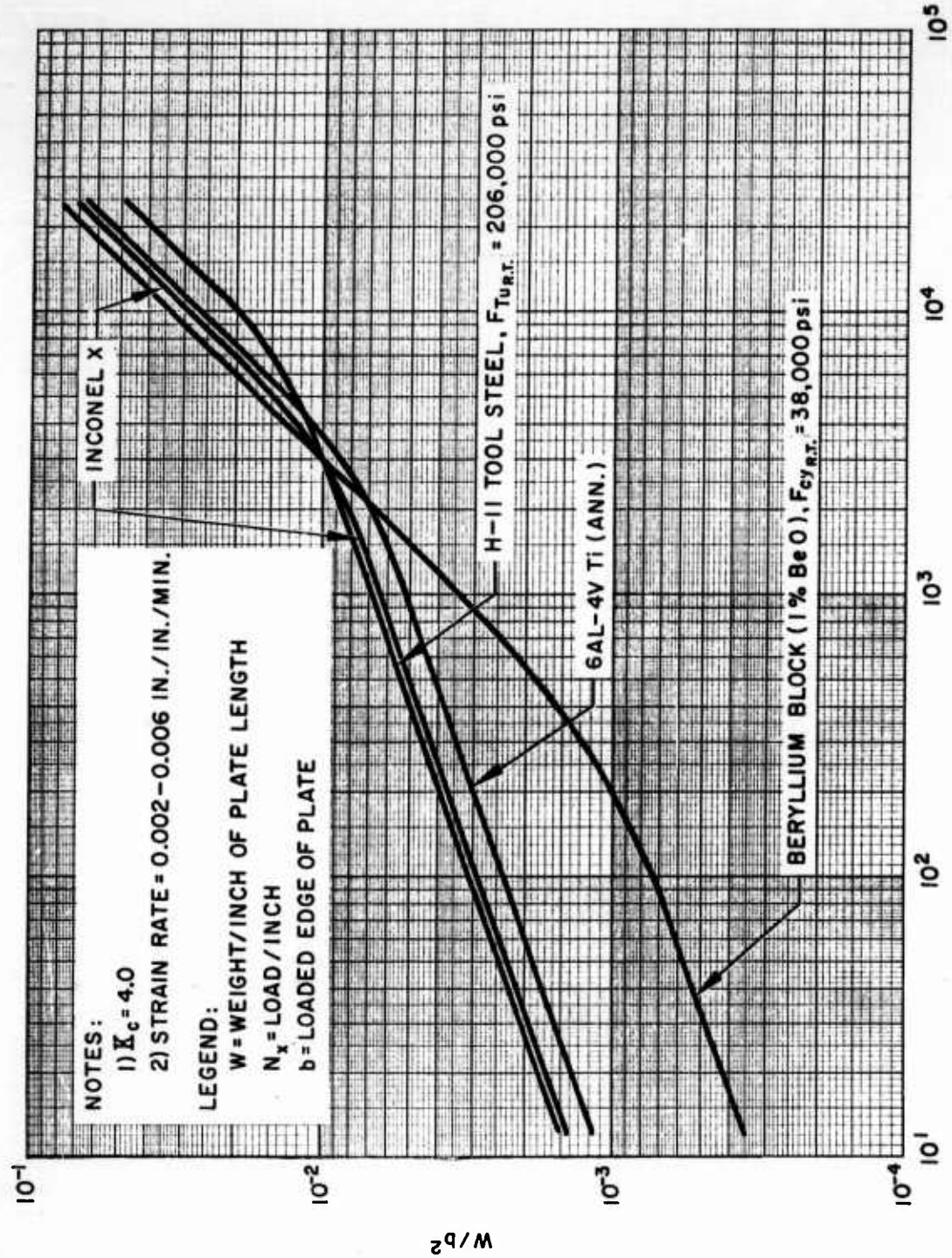

Fig. A-5 Strength-Weight Comparison of Various Sheet Alloys When Used as Flat, Unstiffened Plates in Compression at 1000°F After 0.5 Hour Exposure

Appendix B

SUMMARY OF WIDE-COLUMN, MINIMUM-WEIGHT ANALYSES FOR STIFFENED CONSTRUCTIONS

B.1 GENERAL

This appendix presents a summary of minimum weight analyses of wide-column, stiffened constructions. Two modes of instability – local and wide column – are discussed. When the buckling stresses for these two modes are equated, minimum weight designs may be determined by methods similar to those presented in the body of the report. The buckling stress for local instability can be predicted with Eq. (2.7). The buckling stress for wide-column instability can be predicted with Eq. (B.1), which is the familiar Euler equation:

$$\sigma_E = \frac{\pi^2 \eta_T E}{(\ell'/\rho)^2} \qquad \text{(B.1)}$$

where ρ is the radius of gyration of the wide-column cross-section, and ℓ' is the effective length. It is generally assumed that the wide-column has a sufficient number of stiffeners parallel to the load to allow the panel geometric properties $\bar{t}$ and ρ to be based on a repetitious width b_s even though the end bays may be of width b_s. Wide-column analysis assumes the unloaded edges are free. It may be applied, however, to panels supported along their unloaded edges, if the panel width is of such magnitude that the conditions along the unloaded edges of the panel do not affect panel strength.

The case of an unstiffened wide-column is easily derived by substituting ρ for a flat plate into Eq. (B.1), and taking

$$\frac{N_x}{\ell \eta_T E} = \frac{\sigma}{\eta_T E} \cdot \frac{\bar{t}}{\ell} \qquad \text{(B.2)}$$

$$\sigma_{cr_L} = \sigma_E = \frac{N_x}{\bar{t}} \qquad \text{(B.3)}$$

Equation (B.4) results:

$$\frac{N_x}{\ell \bar{\eta} E} = 0.823 \left(\frac{\bar{t}}{\ell}\right)^3 \text{, where } \bar{\eta} = \eta_T \qquad \text{(B.4)}$$

Note that Eq. (B.4) is in the form of Eq. (2.1). This is, of course, not unexpected in an unstiffened plate. However, it may be shown that all stiffened wide columns having stiffening elements parallel to the load and conforming to the above assumptions also resolve to a minimum weight equation of the form of Eq. (2.1). Thus, combining Eqs. (2.7), (B.1), (B.2) and (B.3), it is determined that

$$\frac{N_x}{\ell \bar{\eta} E} = \mathcal{E} \left(\frac{\bar{t}}{\ell}\right)^2 \qquad \text{(B.5)}$$

where

$$\mathcal{E} = \frac{\rho}{\bar{t}} \frac{\sqrt{K_S}\, \pi^2}{\sqrt{12 (1 - \mu^2)}} \left(\frac{t_s}{b_s}\right) \qquad \text{(B.6)}$$

and

$$\bar{\eta} = \sqrt{\eta_L \eta_T}$$

and ρ and $\bar{t}$ are functions of the wide column geometric proportions. Stiffened wide columns, then, may be compared on the basis of their maximum values of $\mathcal{E}$,

and this comparison holds regardless of the load magnitude. Simple support will be assumed along the loaded edges and the notation ℓ will represent this condition. For other conditions along the loaded edges, replace ℓ in the equations that follow with $\ell/\sqrt{c}$.

B.2 WIDE-COLUMN, MINIMUM-WEIGHT ANALYSES APPEARING IN THE LITERATURE

A number of constructions are treated in the literature. For the purposes of this Appendix it seems desirable to limit those presented to constructions which are discussed in the main body of this report (those which have relatively minor variations in both construction and maximum efficiency are deleted). The constructions discussed are as follows:

(1) Zee-stiffened wide column
(2) Unflanged integrally-stiffened wide column
(3) Truss-core sandwich wide column

The same nomenclature is used for the constructions here as used elsewhere in this report.

B.2.1 Zee-Stiffened Wide Column

This construction has been treated both theoretically and experimentally, with good agreement between results of the two approaches. The minimum-weight analysis results presented here are based on the theoretical approach of Farrar, which is summarized in Ref. 10. From this reference it may be shown that

$$\mathcal{E}_{max} = 0.911$$

$$\left(\frac{t_w}{t_s}\right)_{opt.} = 1.06$$

$$\left(\frac{b_w}{b_s}\right)_{opt.} = 0.87$$

A chart showing these values and other values of these parameters is presented in Fig. B-1. From this figure it may be noted that considerable variation in the parameters may be experienced with little change in maximum efficiency. Figure B-1 has been derived from another form of presentation and is not as accurate as other figures of this type presented previously. It should be noted that the ratio b_f/b_w is taken as 0.3 here. This is quite close to the relationship used in Section 2 of this report for zee-stiffened panels. A value of $b_f/b_w = 0.5$ has also been investigated in Ref. 10, and it is shown that $\mathcal{E}_{max}$ in this case is reduced to 0.760. It may be surmised that this decreased value of $\mathcal{E}$ is the result of decreased local instability stresses in the free flange even though the radius of gyration in wide column computations has increased.

The equations to be used with Fig. B-1 in determining the dimensions of a zee-stiffened, wide column, in addition to Eq. (B.5), are:

$$b_f = 0.3\, b_w$$

$$t_f = t_w$$

$$t_s = \frac{\bar{t}}{\left[1 + 1.6\, \frac{b_w}{b_s} \cdot \frac{t_w}{t_s}\right]}$$

$$\frac{b_w}{\ell} = \frac{0.4\left(1 + 1.6\, \frac{b_w}{b_s} \cdot \frac{t_w}{t_s}\right)}{\sqrt{\frac{b_w}{b_s} \cdot \frac{t_w}{t_s}\left(1 + 0.59\, \frac{b_w}{b_s} \cdot \frac{t_w}{t_s}\right)}} \sqrt{\frac{\frac{N_x}{\ell \eta_T E}}{\bar{t}/\ell}}$$

$$\bar{\eta} = \left[\eta_T\right]^{3/4}$$

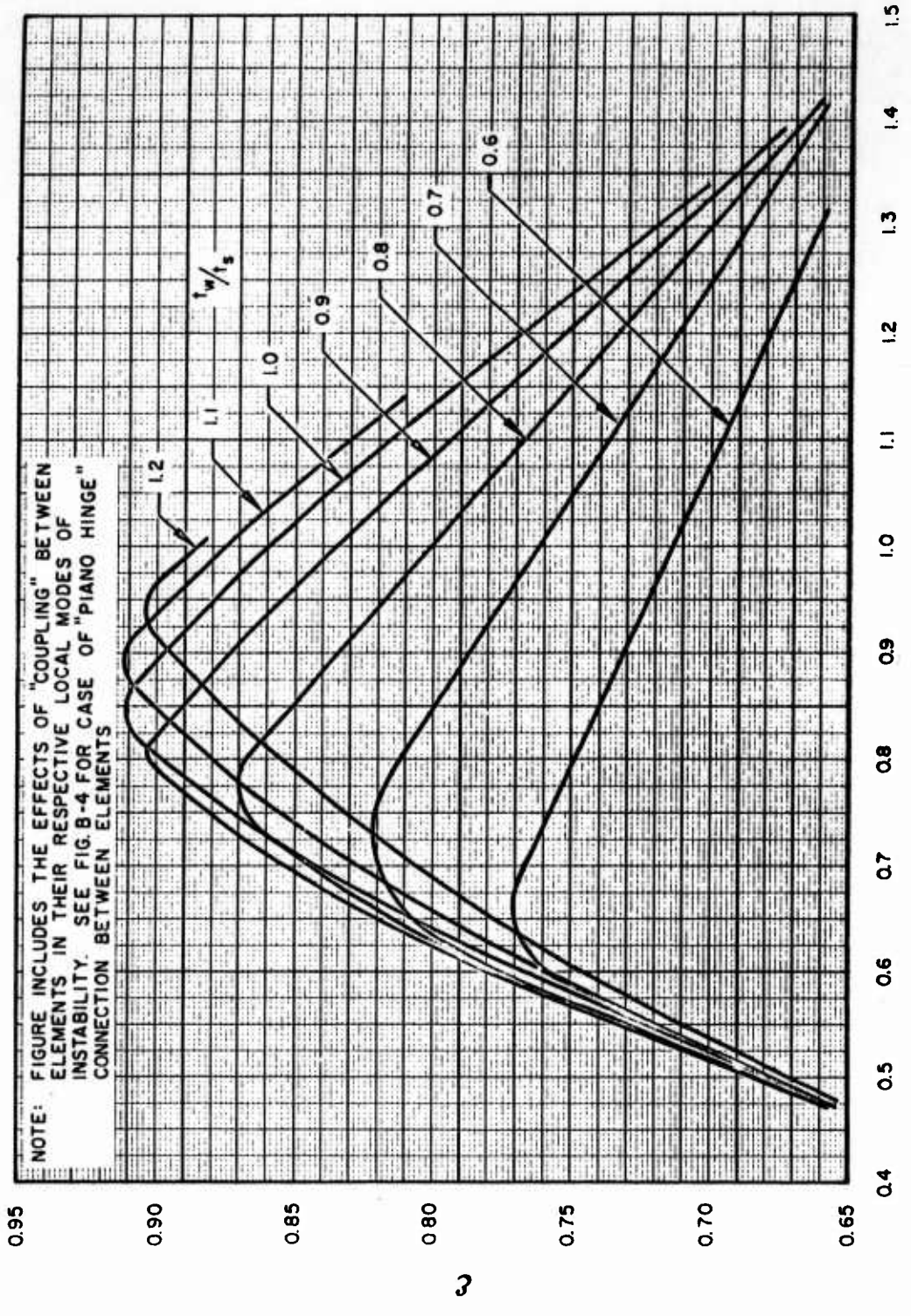

Fig. B-1 Efficiency Chart for Zee-Stiffened Wide Columns

Values of $\mathcal{E}_{max}$ for hat-stiffened wide columns and Y-stiffened wide columns may also be derived from information presented in Ref. 10.

B.2.2 Unflanged Integrally-Stiffened Wide Column

Catchpole (Ref. 11) has made a minimum weight analysis of unflanged integrally-stiffened wide columns with the following results:

$$\mathcal{E}_{max} = 0.656$$

$$\left(\frac{t_w}{t_s}\right)_{opt.} = 2.25$$

$$\left(\frac{b_w}{b_s}\right)_{opt.} = 0.65$$

These values may be obtained from the efficiency chart for this construction (Fig. B-2) which shows, again, that the peak of the efficiency curve is rather flat and that a wide range of values of the above parameters yields approximately the same maximum efficiency. Equations to be used with Fig. B-2 to determine the dimensions of the design, in addition to Eq. (B.5), are:

$$\frac{b_s}{\ell} = 1.1\left[1 + \frac{t_w}{t_s}\cdot\frac{b_w}{b_s}\right]\sqrt{\frac{\frac{N_x}{\ell\eta_T E}}{\frac{\bar{t}}{\ell}\left[\frac{t_w}{t_s}\left(\frac{b_w}{b_s}\right)^3\right]\left[4 + \frac{t_w}{t_s}\frac{b_w}{b_s}\right]}}$$

$$t_s = \frac{\bar{t}}{\left[1 + \frac{t_w}{t_s}\cdot\frac{b_w}{b_s}\right]}$$

$$\bar{\eta} = \left[\eta_T\right]^{3/4}$$

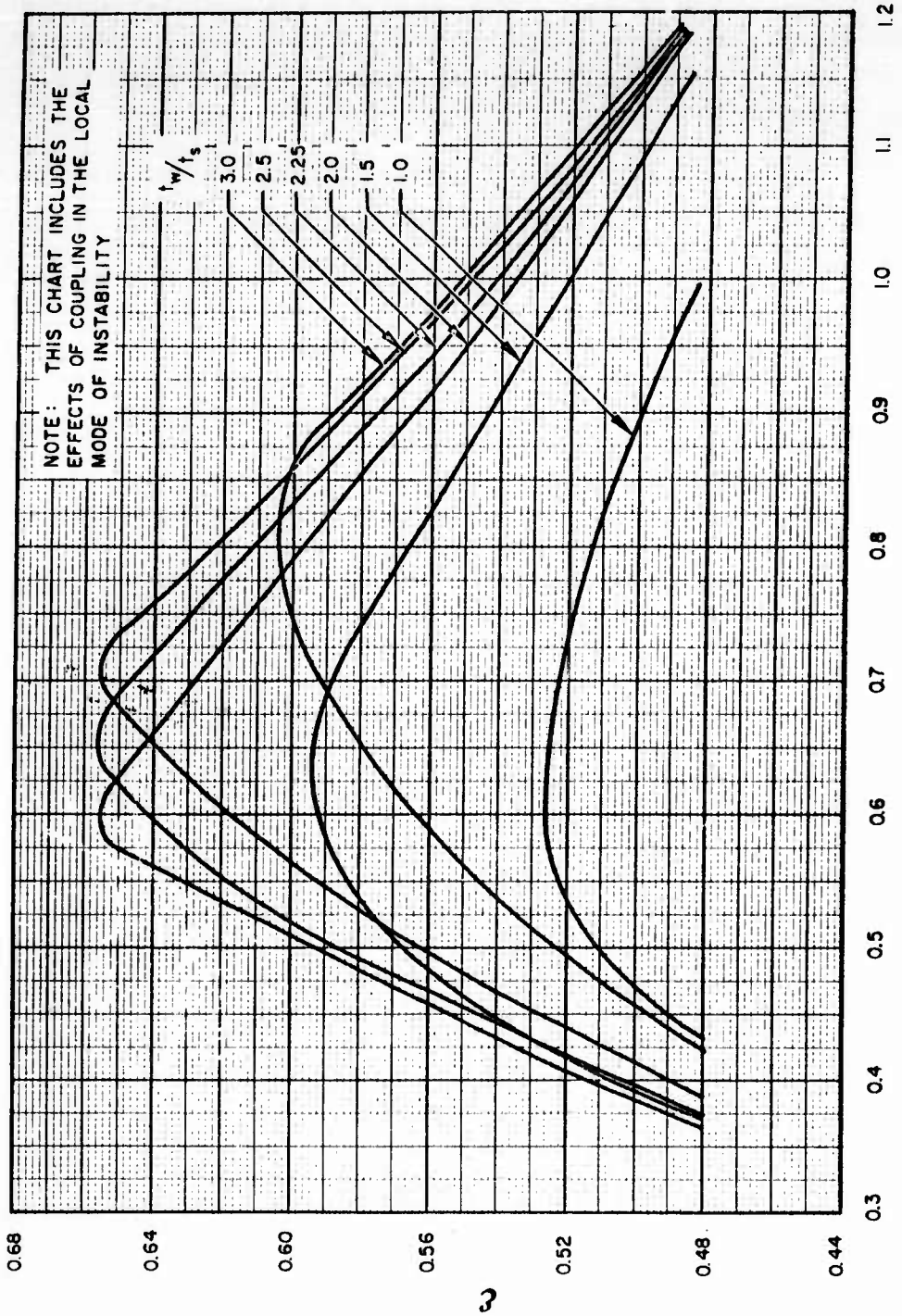

Fig. B-2 Efficiency Chart for Unflanged, Integrally-Stiffened Wide Columns

As in the previous construction presented, Fig. B-2 has been derived from a different form of presentation and the level of accuracy is not as high as in charts of this type in the body of this report.

B.2.3 Truss-Core Sandwich Wide Column

The truss-core, sandwich wide column has been optimized in Ref. 3. It is shown in this reference that:

$$\mathcal{E}_{max} = 0.605$$

$$\theta_{opt.} = 62°$$

$$\left(\frac{t_c}{t_f}\right)_{opt.} = 0.92$$

While the minimum weight equation for this construction is represented by Eq. (B.5), it holds true only when $\bar{t}/\ell$ is less than 10^{-2}. Above this value of $\bar{t}/\ell$, shear-stiffness effects in the sandwich cannot be neglected and their inclusion complicates the simple form of Eq. (B.5) considerably.

An efficiency chart for this construction is shown as Fig. B-3. Equations to be used with this chart and Eq. (B.5), keeping in mind the limitation mentioned above, are:

$$\frac{t_f}{\ell} = \frac{\frac{\bar{t}}{\ell}}{2 + \frac{t_c}{t_f}\,\frac{1}{\cos\,\theta}}$$

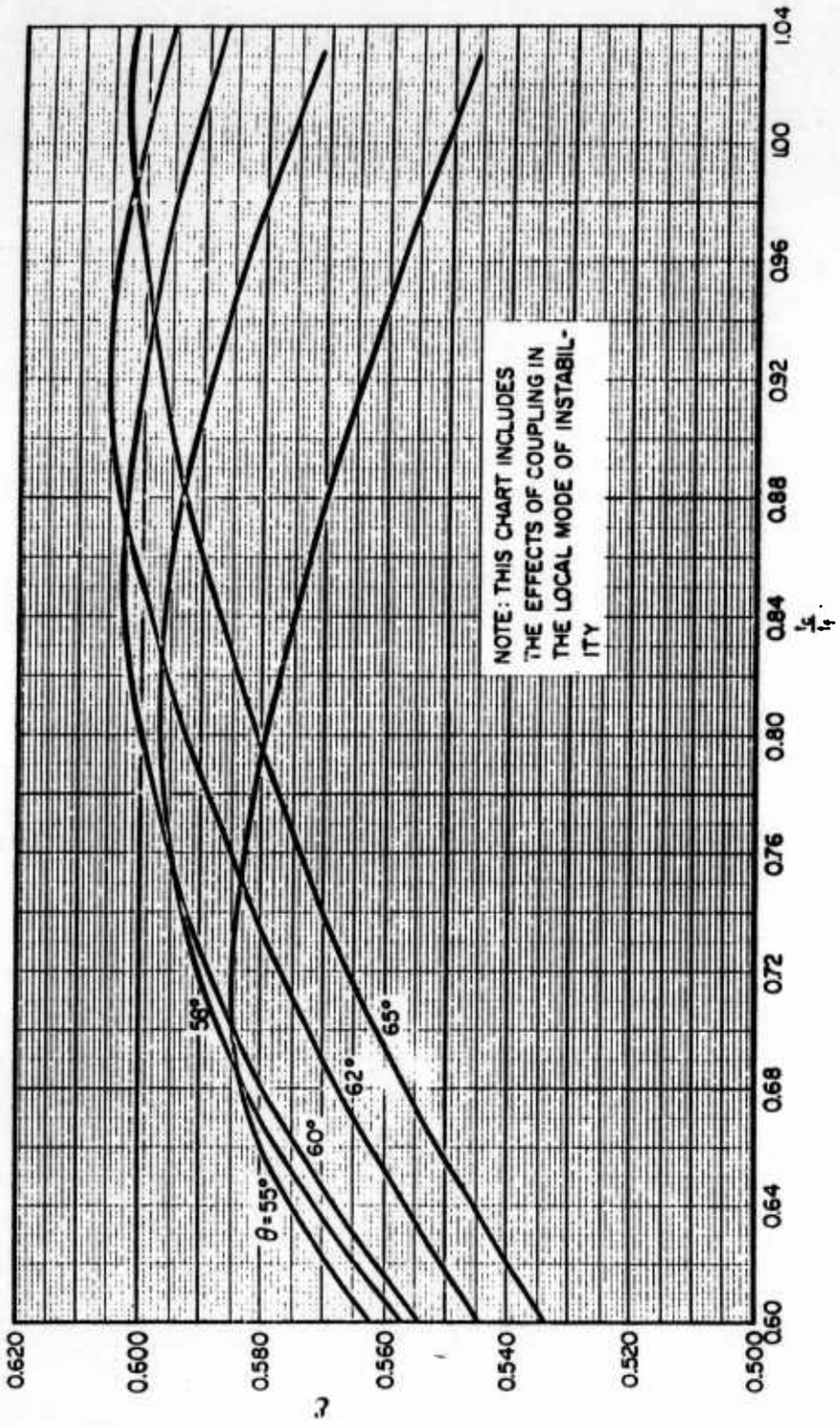

Fig. B-3 Efficiency Chart for Truss-Core Sandwich Wide Columns

$$b_f = 0.95\, t_f \sqrt{\frac{K_X\left(\frac{\bar{t}}{\ell}\right)}{\frac{N_x}{\ell \cdot \eta_L E}}}$$

where $\eta_L = \sqrt{\eta_T}$; K_X is taken from Ref. 6.

$$b_c = \frac{b_f}{2 \cos \theta}$$

In this construction, the value of $\bar{\eta}$ in Eq. (B.5) is represented by:

$$\bar{\eta} = \sqrt{\frac{2\eta_T\, 3/2}{1 + \eta_T}}$$

B.3 THE EFFECT OF COUPLING IN THE LOCAL INSTABILITY MODE ON THE MAXIMUM EFFICIENCY OF STIFFENED, WIDE COLUMNS

Coupling as used here is defined as the mutual restraint between adjoining elements in their respective local modes of instability.

In the body of this report, it is assumed, for the zee-stiffened panels and the unflanged, integrally-stiffened panels, that there is a "piano-hinge" connection between adjoining elements which is a conservative assumption when the uncoupled critical stresses of skin and stiffener are approximately equal. In contrast, the wide-column minimum weight analyses presented in the foregoing paragraphs include the effects of coupling in the local mode of instability. Charts of buckling coefficients, including the effects of coupling, are presented in the literature (see Figs. 2.2-9 through 2.2-11 in Ref. 4, for example). These charts were not considered in the panel analyses of this report because of the added complexity to already lengthy analyses compared to the wide column analyses. Nonetheless, it is of interest to determine the effect, if any, on the

maximum efficiency of a stiffened wide column, of neglecting the coupling effects in the local mode of instability.

The construction chosen for this comparison is the zee-stiffened, wide-column construction. From previous discussion, it is apparent that Eqs. (B.5) and (B.6) are applicable. The result of the piano hinge connections between adjoining elements may be stated as follows:

$$\mathcal{E} = 5.98 \frac{\rho}{\bar{t}} \left(\frac{t_s}{b_s} \right)$$

$$b_f = 0.3535\, b_w$$

$$\frac{t_w}{t_s} = \frac{b_w}{b_s}$$

$$t_f = t_w$$

If $\bar{t}$ and ρ are based on a unit repetitive width and if it is assumed: (1) the half thickness of the skin and flange are negligible in comparison to the stiffener web height, and (2) the moments of inertia of the skin and flanges about their own midplane axis are negligible in comparison to the moment of inertia of the unit repetitive width of the wide-column, the following equations result:

$$\bar{t} = \frac{1.707\, t_w\, b_w + b_s\, t_s}{b_s}$$

$$\rho = \frac{b_w \sqrt{0.442 + 0.6868 \frac{b_s}{b_w} \cdot \frac{t_s}{t_w}}}{\left[1.707 + \frac{t_s}{t_w} \cdot \frac{b_s}{b_w} \right]}$$

Substituting

$$\mathcal{E} = \frac{3.97 \frac{b_s}{b_w} \sqrt{1 + 1.555 \left(\frac{b_s}{b_w}\right)^2}}{\left[1.707 + \left(\frac{b_s}{b_w}\right)^2\right]^2} \qquad \text{(B.7)}$$

A graphical solution to Eq. (B.7) is presented in Fig. B-4. From this figure it is determined that

$$\mathcal{E}_{max} = 0.871$$

$$\left(\frac{b_w}{b_s}\right)_{opt.} = 0.90$$

The above equations are sufficient to determine dimensions in a given design when the following equations are also known:

$$t_s = \frac{\bar{t}}{1 + 1.707 \left(\frac{b_w}{b_s}\right)^2}$$

$$b_s = 1.902\, t_s \sqrt{\frac{\frac{\bar{t}}{\ell}}{\frac{N_x}{\ell \eta_L E}}} \quad , \quad \text{where} \quad \eta_L = \sqrt{\eta_T}$$

$$\bar{\eta} = \left[\eta_T\right]^{3/4}$$

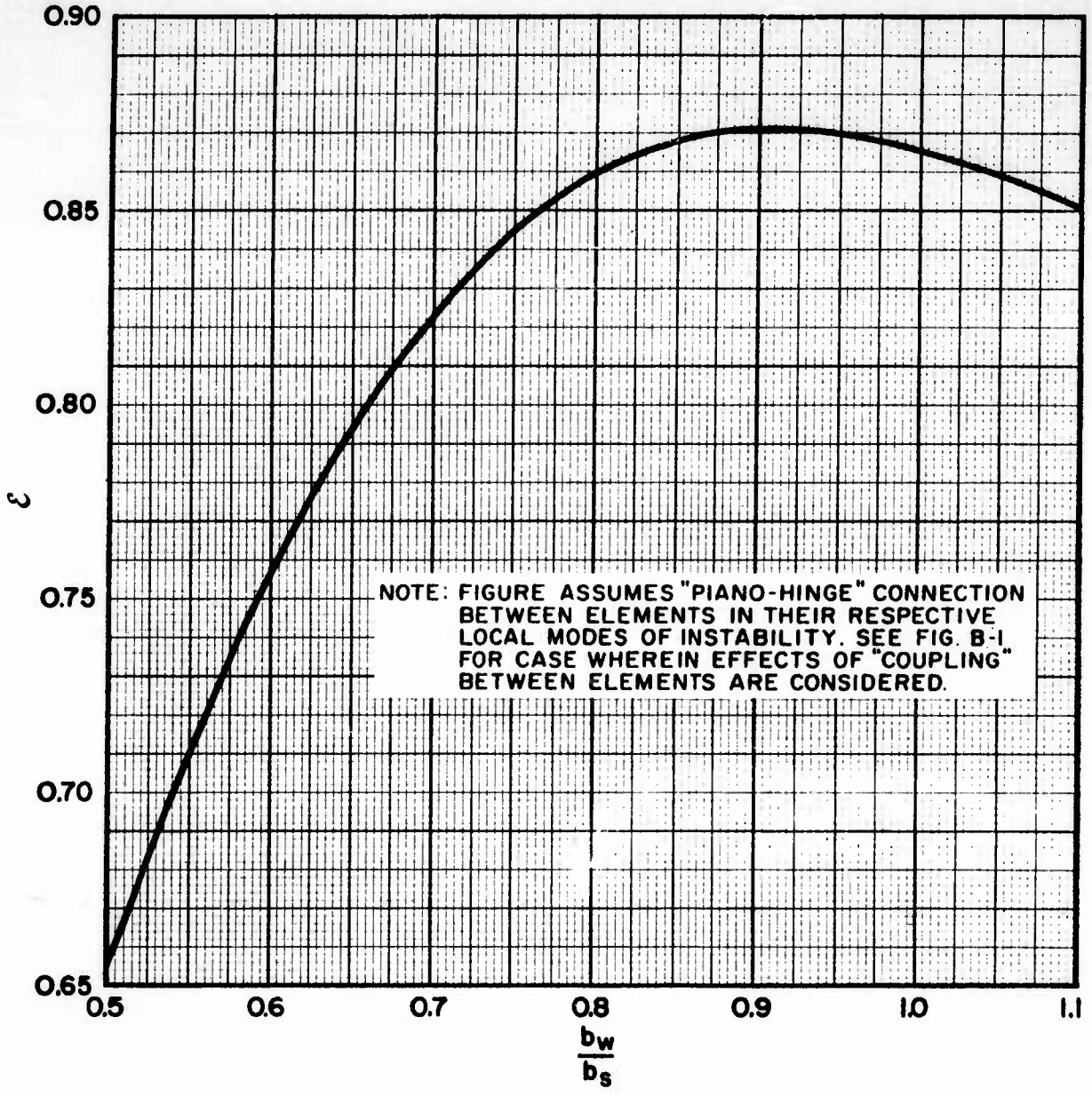

Fig. B-4 Efficiency Chart for Zee-Stiffened Wide Columns

A comparison of $\mathcal{E}_{max}$ for the present analysis to that for the analysis where coupling in the local mode of instability is considered shows the latter analysis to be approximately 4 percent more efficient. In view of the assumptions and approximations involved, the difference in the two solutions is negligible.

A comparison of the optimum, geometric parameters derived from the two analyses shows $(b_w/b_s)_{opt.}$ to be about the same in both cases. The values of $(t_w/t_s)_{opt.}$ show some difference owing to incomparable values of the local buckling coefficient K_S. Note that the assumption of piano-hinge connection between adjoining elements in the local mode of instability results in a simpler solution, $\mathcal{E}$ being in terms of a single parameter. The conclusion to be reached from this comparison appears to be that coupling between adjoining elements in their respective local modes of instability need not be considered in order to develop a reasonably accurate value of $\mathcal{E}_{max}$.

B.4 THE MAXIMUM ATTAINABLE $\mathcal{E}$ FOR WIDE COLUMNS

From the stiffened, wide-column constructions considered thus far, it would appear that the maximum attainable $\mathcal{E}$ for the condition imposed, i.e., failure occurring with the first buckle, is in the vicinity of unity. It would also appear, from Euler column experience, that the efficiency of the wide column will improve as the cross-section approaches an I-beam configuration. This speculation is supported by the increase in $\mathcal{E}_{max}$ from the unflanged integrally-stiffened geometry to the zee-stiffened geometry.

The literature (Ref. 12) contains a wide-column minimum weight analysis for a prismoidal sandwich construction possessing an I-beam geometry in its unit repetitive width (Fig. B-5). The analysis assumes piano-hinge connection between adjoining elements in their respective local modes of instability.

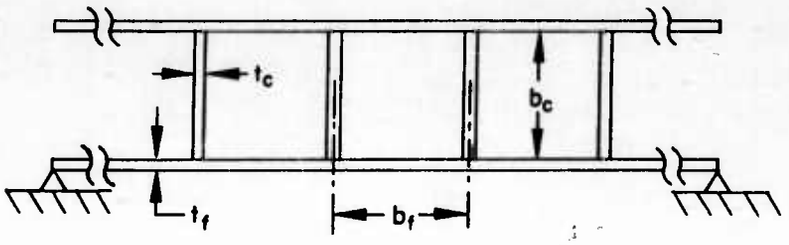

Fig. B-5 Cross-Sectional Geometry of a Prismoidal Sandwich Wide Column

The analysis yields:

$$\mathcal{E}_{max} = 0.886$$

$$\left(\frac{t_c}{t_f}\right)_{opt.} = 1.136$$

where

$$\frac{t_c}{t_f} = \frac{b_c}{b_f}$$

An efficiency chart for this construction is presented in Fig. B-6. In addition to Eq. (B.5), the following equations are used to calculate the dimensions of a design:

$$t_f = \frac{\bar{t}}{2 + \left(\frac{b_c}{b_f}\right)^2}$$

$$b_f = 1.902\, t_f \sqrt{\frac{\bar{t}/\ell}{\frac{N_x}{\ell \eta_L E}}} \quad , \quad \text{where } \eta_L = \sqrt{\eta_T}$$

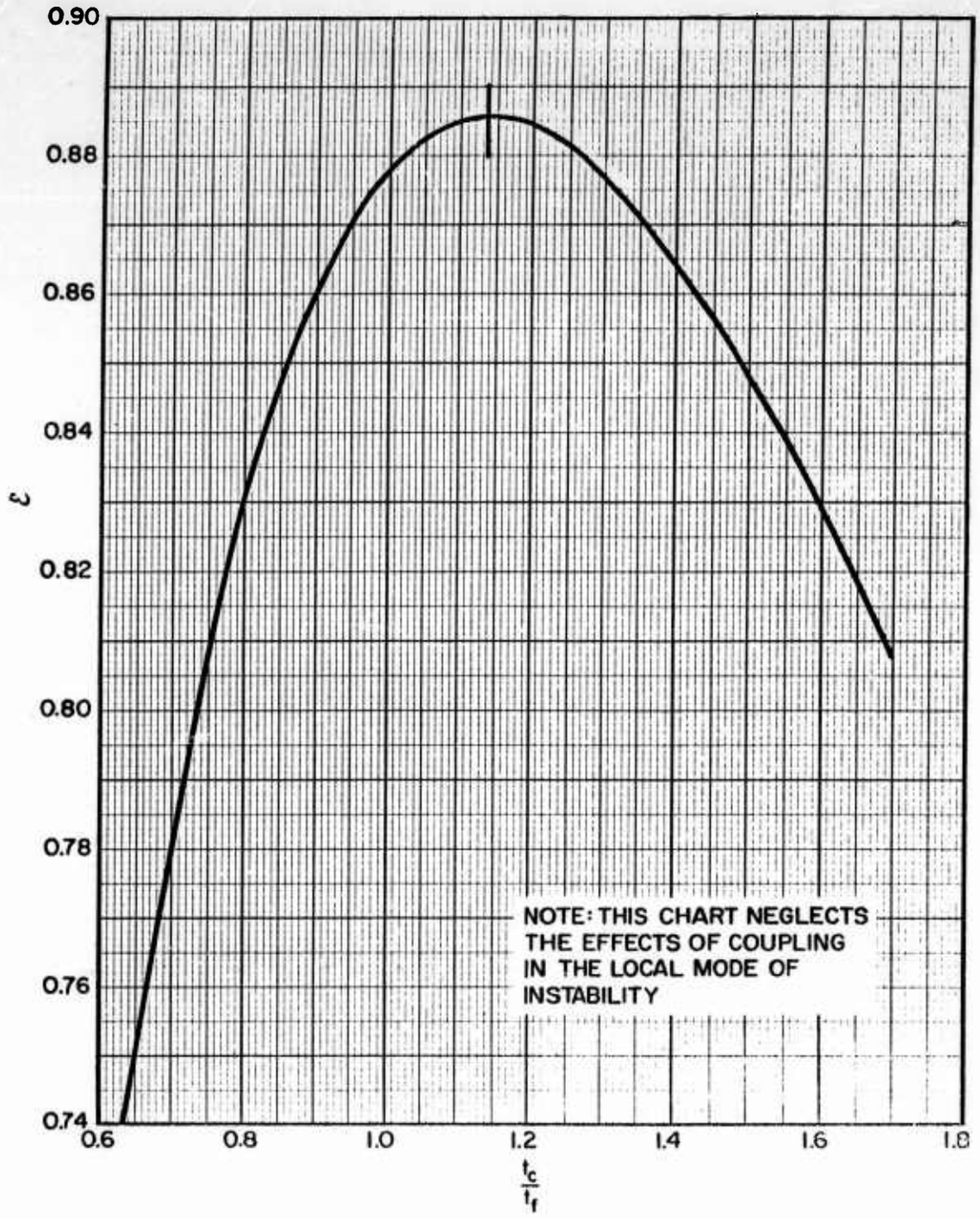

Fig. B-6 Efficiency Chart for Prismoidal Sandwich Wide Columns

$$\bar{\eta} = \left[\eta_T\right]^{3/4}$$

Comparing $\mathcal{E}_{max}$ for the prismoidal sandwich wide column to that for the proper zee-stiffened wide column, it is seen that the prismoidal sandwich efficiency is two percent higher. This seems to indicate that the zee stiffener is a near-optimum stiffener geometry for use in conventionally stiffened wide columns. It would also seem that the maximum attainable value of $\mathcal{E}$, based on piano-hinge connections between adjoining elements in their respective local modes of instability, would be limited to approximately 0.90 for any geometry.

While the prismoidal sandwich construction is not a practical structure from a manufacturing point of view, or, for a lateral loading, it does represent a highly efficient construction for application as a wide column and has been useful in drawing conclusions as to the magnitude of the maximum efficiencies obtainable.

B.5 THE RELATIVE EFFICIENCIES OF WIDE-COLUMN, STIFFENED, PANEL CONSTRUCTIONS

The results of the wide-column, minimum-weight analyses presented in this appendix are compared in Fig. B-7. It is apparent from this figure that the stiffened panel constructions are far superior to the flat, unstiffened wide column regardless of the type of stiffener. Further, the differences between the stiffened, wide-column designs considered are not too significant. It may be concluded that the zee-stiffener design is the most efficient among the practical stiffening elements shown. The chart also indicates, as concluded previously, that consideration of the effects of coupling between adjoining elements in their respective local modes of instability does not yield a significant increase in the efficiency of zee-stiffened panels in comparison to the efficiency determined when these effects are neglected.

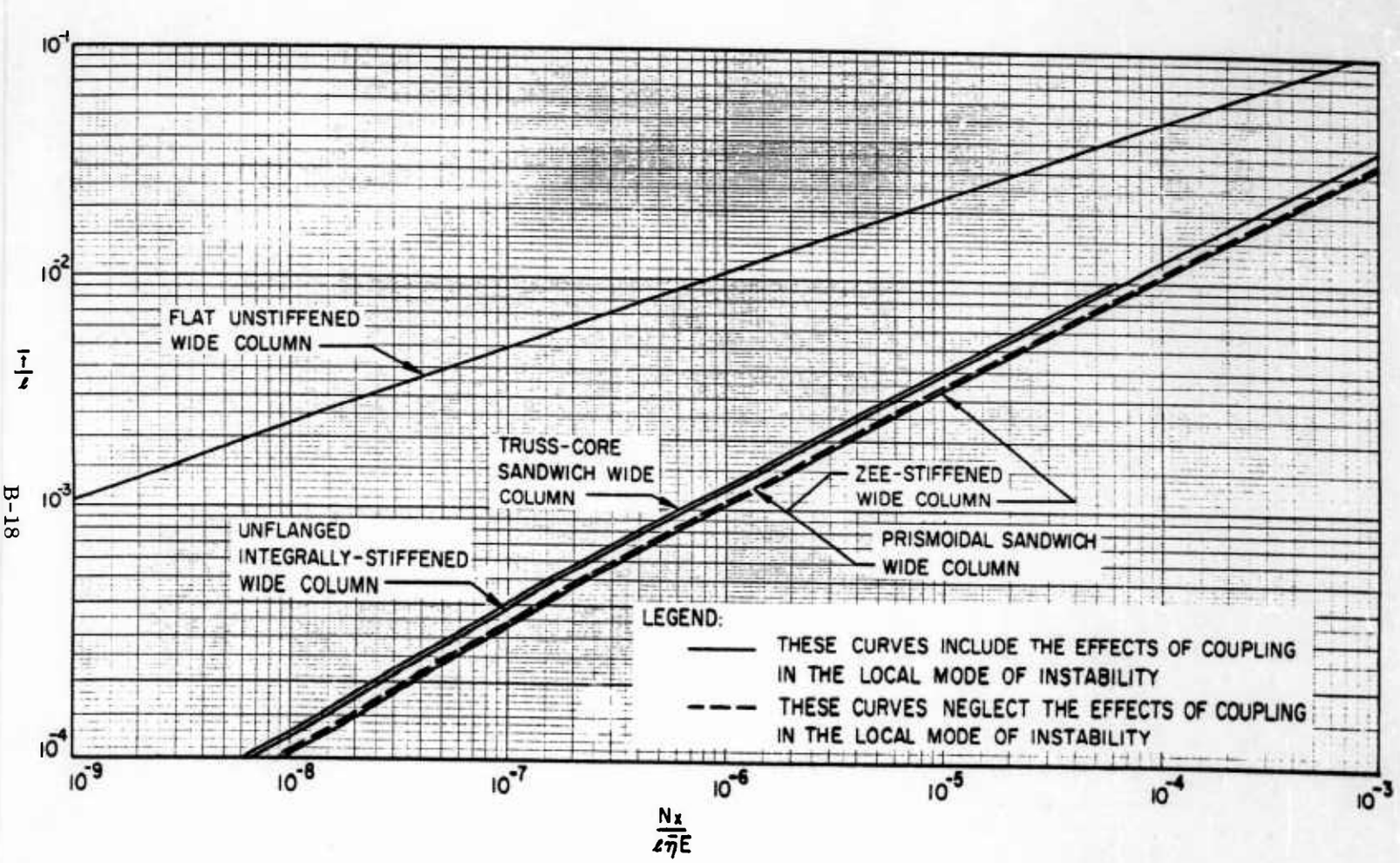

Fig. B-7 Comparison of the Minimum-Weight Envelopes of Several Types of Stiffened, Wide-Column Construction When Subjected to a Compression Load in the Direction of the Stiffening Elements

UNCLASSIFIED